

**Two-body  $B_c \rightarrow D_{(s)}^{(*)}P, D_{(s)}^{(*)}V$  decays in the perturbative QCD approach**

Zhou Rui, Zhi-Tian Zou, and Cai-Dian Lü

*Institute of High Energy Physics and Theoretical Physics Center for Science Facilities, Chinese Academy of Sciences, Beijing 100049, People's Republic of China*

(Received 13 December 2011; published 8 October 2012)

We make a systematic investigation on the two-body nonleptonic decays  $B_c \rightarrow D_{(s)}^{(*)}P, D_{(s)}^{(*)}V$ , by employing the perturbative QCD approach based on  $k_T$  factorization, where  $P$  and  $V$  denote any light pseudoscalar meson and vector meson, respectively. We predict the branching ratios and direct  $CP$  asymmetries of these  $B_c$  decays and also the transverse polarization fractions of  $B_c \rightarrow D_{(s)}^{(*)}V$  decays. It is found that the nonfactorizable emission diagrams and annihilation-type diagrams have remarkable effects on the physical observables in many channels, especially the color-suppressed and annihilation-dominant decay modes. A possible large direct  $CP$  violation is predicted in some channels; and a large transverse polarization contribution which can reach 50%  $\sim$  70% is predicted in some of the  $B_c \rightarrow D_{(s)}^{(*)}V$  decays.

DOI: [10.1103/PhysRevD.86.074008](https://doi.org/10.1103/PhysRevD.86.074008)

PACS numbers: 13.25.Hw, 12.38.Bx, 14.40.Nd

**I. INTRODUCTION**

The  $B_c$  meson is the only quark-antiquark bound system ( $\bar{b}c$ ) composed of both heavy quarks with different flavors, and are thus flavor-asymmetric. It can decay only via weak interaction, since the two-flavor asymmetric quarks ( $b$  and  $c$ ) cannot annihilate into gluons or photons via strong interaction or electromagnetic interaction. Because each of the two heavy quarks can decay individually, and they can also annihilate through weak interaction,  $B_c$  meson has rich decay channels and provides a very good place to study nonleptonic weak decays of heavy mesons to test the standard model and to search for any new physics signals [1].

Since the current running LHC collider will produce much more  $B_c$  mesons than ever before, a lot of theoretical studies of the nonleptonic  $B_c$  weak decays have been performed using different approaches—for example, the spectator model [2], the light-front quark model (LFQM) [3,4], the relativistic constituent quark model (RCQM) [5], the QCD factorization approach [6], the Perturbative QCD approach (pQCD) [7–10], and so on. Among the numerous decay channels, there is one category with only one charmed meson in the final states. They are rare decays, but with possible large direct  $CP$  asymmetry, since there are both penguin and tree diagrams involved. These decays have been studied in Ref. [3] using the naive factorization approach. But they consider only the contribution of current-current operators at the tree level, and thus no direct  $CP$  asymmetry is predicted. They also have difficulty predicting those pure penguin-type or annihilation-dominant-type decays, such as  $B_c \rightarrow D^+\phi, D_s^+\bar{K}^0, D_s^+\phi$ . Reference [5] discussed some semileptonic and nonleptonic  $B_c$  weak decays and  $CP$ -violating asymmetries by using the RCQM model based on the Bethe-Salpeter formalism. They do not include the contributions of annihilation-type

diagrams, either. Since the annihilation-type contributions are found to be important in the  $B$ -meson nonleptonic decays [11] and also significant in the  $B_c$  decays [12], one needs to further study these channels carefully.

In this paper, we calculate all the processes of a  $B_c$ -meson decay to one  $D_{(s)}^{(*)}$  meson and one light pseudoscalar meson ( $P$ ) or vector meson ( $V$ ) in the pQCD approach. It is well-known that the  $B_c$  meson is a nonrelativistic heavy quarkonium system. Thus, the two quarks in the  $B_c$  meson are both at rest and nonrelativistic. Since the charm quark in the final-state  $D$  meson is almost at collinear state, a hard gluon is needed to transfer large momentum to the spectator charm quark. In the leading order of  $m_c/m_{B_c} \sim 0.2$  expansion, the factorization theorem is applicable to the  $B_c$  system similar to the situation of the  $B$  meson [13]. Utilizing the  $k_T$  factorization instead of collinear factorization, this approach is free of endpoint singularity. Thus, the diagrams including factorizable, nonfactorizable, and annihilation type are all calculable. It has been tested in the study of charmless  $B$ -meson decays successfully [14], especially for the direct  $CP$  asymmetries [15]. For the charmed decays of the  $B$  meson, it is also demonstrated to be applicable in the leading order of the  $m_D/m_B$  expansion [16–21].

Our paper is organized as follows: We review the pQCD factorization approach and then perform the perturbative calculations for these considered decay channels in Sec. II. The numerical results and discussions on the observables are given in Sec. III. The final section is devoted to our conclusions. Some details related functions and the decay amplitudes are given in Appendixes A and B.

**II. THEORETICAL FRAMEWORK**

For the charmed  $B_c$  decays we considered, the weak effective Hamiltonian  $\mathcal{H}_{\text{eff}}$  for  $b \rightarrow q'(q' = d, s)$  transition can be written as [22]

\*lucd@ihep.ac.cn

$$\mathcal{H}_{\text{eff}} = \frac{G_F}{\sqrt{2}} \left\{ \sum_{q=u,c} \xi_q [(C_1(\mu)O_1^q(\mu) + C_2(\mu)O_2^q(\mu)) + \sum_{i=3}^{10} C_i(\mu)O_i(\mu)] \right\}, \quad (1)$$

with the Cabbibo-Kobayashi-Maskawa (CKM) matrix element  $\xi_q = V_{qq'}V_{qb}^*$ .  $O_i(\mu)$  and  $C_i(\mu)$  are the effective four quark operators and their QCD corrected Wilson coefficients, respectively. Their expressions can be found easily, for example, in Ref. [22].

With these quark-level weak operators, the hardest work is left for the matrix element calculation between hadronic states  $\langle DM | H_{\text{eff}} | B_c \rangle$ . Since both perturbative and nonperturbative QCD are involved, the factorization theorem is required to make the calculation meaningful. The perturbative QCD approach [14] is one of the methods to deal with hadronic B decays based on  $k_T$  factorization. At zero recoil of the  $D$  meson in the semileptonic  $B_c$  decay, both  $c$  and  $b$  quark can be described by heavy quark effective theory. However, when the  $D$  meson is at maximum recoil, which is the case of two-body nonleptonic  $B_c$  decay, the final-state mesons, so as to the constituent quarks ( $c$  and other light quarks) inside, at the rest frame of the  $B_c$  meson are collinear. Since the spectator  $c$  quark in the  $B_c$  meson is almost at rest, a hard gluon is then needed to transform it into a collinear object in the final-state meson. This makes the perturbative calculations into a six-quark interaction. In this collinear factorization calculation, endpoint singularity usually appears in some of the diagrams. The QCD factorization approach [23] just parameterizes those diagrams with singularity as free parameters; while in the so-called soft-collinear effective theory [24], people separate these incalculable parts to an unknown matrix element. In our pQCD approach, we studied these singularities and found that they arise from the endpoint where longitudinal momentum is small. Therefore, the transverse momentum of quarks is no longer negligible. If one picks back the transverse momentum, the result is finite.

Because the intrinsic transverse momentum of quarks is smaller than the  $b$  quark mass scale, we have one more scale than the usual collinear factorization. Additional double logarithms appear at the perturbative QCD calculations. These large logarithms will spoil the perturbation expansion; thus, a resummation is required. This has been done to give the so-called Sudakov form factors [25]. The single logarithm between the W boson mass scale and the factorization scale  $t$  in the pQCD approach has been absorbed into the Wilson coefficients of four quark operators. The decay amplitude is then factorized into the convolution of the hard subamplitude, the Wilson coefficient, and the Sudakov factor with the meson wave functions, all of which are well-defined and gauge-invariant. Therefore, the three-scale factorization formula for exclusive nonleptonic  $B$ -meson decays is then written as

$$C(t) \otimes H(x, t) \otimes \Phi(x) \otimes \exp \left[ -s(P, b) - 2 \int_{1/b}^t \frac{d\mu}{\mu} \gamma_q(\alpha_s(\mu)) \right], \quad (2)$$

where  $C(t)$  are the corresponding Wilson coefficients. The Sudakov evolution  $\exp[-s(P, b)]$  [25] are from the resummation of double logarithms  $\ln^2(Pb)$ , with  $P$  denoting the dominant light-cone component of meson momentum.  $\gamma_q = -\alpha_s/\pi$  is the quark anomalous dimension in axial gauge. All nonperturbative components are organized in the form of hadron wave functions  $\Phi(x)$ , which can be extracted from experimental data or other nonperturbative methods. Since nonperturbative dynamics has been factored out, one can evaluate all possible Feynman diagrams for the six-quark amplitude straightforwardly, which include both traditional factorizable and so-called nonfactorizable contributions. Factorizable and nonfactorizable annihilation-type diagrams are also calculable without endpoint singularity.

The meson wave function, which describes hadronization of the quark and antiquark inside the meson, is independent of the specific processes. Using the wave functions determined from other well-measured processes, one can make quantitative predictions here. For the light pseudo-scalar meson, its wave function can be defined as [26]

$$\Phi(P, x, \xi) = \frac{i}{2N_c} \gamma_5 [\not{P} \phi_P^A(x) + m_0 \phi_P^P(x) + \xi m_0 (\not{v} - 1) \phi_P^T(x)], \quad (3)$$

where  $P$  is the momentum of the light meson, and  $x$  is the momentum fraction of the quark (or antiquark) inside the meson. When the momentum fraction of the quark (antiquark) is set to be  $x$ , the parameter  $\xi$  should be chosen as  $+1(-1)$ . The distribution amplitudes  $\phi_P^A(x)$ ,  $\phi_P^P(x)$ , and  $\phi_P^T(x)$  are given in Appendix C.

For the light vector mesons, both longitudes (L) and transverse (T) polarizations are involved. Their wave functions are written as [7]

$$\begin{aligned} \Phi_V^L(x) &= \frac{1}{\sqrt{2N_c}} \{ M_V \not{\epsilon}_V^{*L} \phi_V(x) + \not{\epsilon}_V^{*L} \not{P} \phi_V^L(x) \\ &\quad + M_V \phi_V^s(x) \}_{\alpha\beta}, \\ \Phi_V^T(x) &= \frac{1}{\sqrt{2N_c}} \{ M_V \not{\epsilon}_V^{*T} \phi_V^V(x) + \not{\epsilon}_V^{*T} \not{P} \phi_V^T(x) \\ &\quad + i M_V \epsilon_{\mu\nu\rho\sigma} \gamma_5 \epsilon_T^{*\nu} n^\rho v^\sigma \phi_V^a(x) \}_{\alpha\beta}, \end{aligned} \quad (4)$$

where  $\epsilon_V^{L(T)}$  denotes the longitudinal (transverse) polarization vector. And convention  $\epsilon^{0123} = 1$  is adopted for the Levi-Civita tensor. The distributions amplitudes are also presented in Appendix C.

Consisting of two heavy quarks ( $b, c$ ), the  $B_c$  meson is usually treated as a heavy quarkonium system. In the non-relativistic limit, the  $B_c$  wave function can be written as [7]

$$\Phi_{B_c}(x) = \frac{if_B}{4N_c} [(\not{p} + M_{B_c})\gamma_5\delta(x - r_c)], \quad (5)$$

with  $r_c = m_c/M_{B_c}$ . Here, we only consider one of the dominant Lorentz structures and neglect another contribution in our calculation [27].

In the heavy quark limit, the two-particle light-cone distribution amplitudes of  $D_{(s)}/D_{(s)}^*$  meson are defined as [21]

$$\begin{aligned} \langle D_{(s)}(P_2) | q_\alpha(z) \bar{c}_\beta(0) | 0 \rangle &= \frac{i}{\sqrt{2N_c}} \int_0^1 dx e^{ixP_2 \cdot z} \\ &\quad \times [\gamma_5(\not{p}_2 + m_{D_{(s)}})\phi_{D_{(s)}}(x, b)]_{\alpha\beta}, \\ \langle D_{(s)}^*(P_2) | q_\alpha(z) \bar{c}_\beta(0) | 0 \rangle &= -\frac{1}{\sqrt{2N_c}} \int_0^1 dx e^{ixP_2 \cdot z} \\ &\quad \times [\not{\epsilon}(\not{p}_2 + m_{D_{(s)}^*})\phi_{D_{(s)}^*}(x, b)]_{\alpha\beta}. \end{aligned} \quad (6)$$

We use the following relations derived from heavy quark effective theory to determine  $f_{D_{(s)}^*}$  [28]:

$$f_{D_{(s)}^*} = \sqrt{\frac{m_{D_{(s)}}}{m_{D_{(s)}^*}}} f_{D_{(s)}}. \quad (7)$$

For the  $D_{(s)}^{(*)}$ -meson wave function, we adopt the same model as of the  $B$  meson [8]

$$\phi_{D_{(s)}}(x, b) = N_{D_{(s)}} [x(1-x)]^2 \exp\left(-\frac{x^2 m_{D_{(s)}}^2}{2\omega_{D_{(s)}}^2} - \frac{1}{2}\omega_{D_{(s)}}^2 b^2\right), \quad (8)$$

with shape parameters  $\omega_D = 0.6$  for the  $D/D^*$  meson and  $\omega_{D_s} = 0.8$  for the  $D_s/D_s^*$  meson. Here, a larger  $\omega_{D_s}$  parameter than  $\omega_D$  characterizes the fact that the  $s$  quark in the  $D_s$  meson carries a larger momentum fraction than the light quark ( $u, d$ ) in the  $D$  meson.

At leading order, there are eight types of diagrams which may contribute to the  $B_c \rightarrow D_{(s)}^{(*)}P, D_{(s)}^{(*)}V$  decays as illustrated in Fig. 1. The first lines are the emission-type diagrams, with the first two contributing to the usual form factor and the last two contributing to the so-called nonfactorizable diagrams. The second lines are the annihilation-type diagrams, with the first two factorizable and the last two nonfactorizable.

### A. Amplitudes for $B_c \rightarrow D_{(s)}^{(*)}P$ decays

We mark LL, LR, and SP to denote the contributions from  $(V-A)(V-A)$ ,  $(V-A)(V+A)$  and  $(S-P)(S+P)$  operators, respectively. The amplitudes from factorizable diagrams (a) and (b) in Fig. 1 are as following:

$$\begin{aligned} \mathcal{F}_e^{\text{LL}} &= 2\sqrt{\frac{2}{3}} C_F f_B f_P \pi M_B^4 \int_0^1 dx_2 \int_0^\infty b_1 b_2 db_1 db_2 \phi_D(x_2, b_2) \{ [(1-2r_D)x_2 \\ &\quad + (r_D-2)r_b] \alpha_s(t_a) h_e(\alpha_e, \beta_a, b_1, b_2) S_f(x_2) \exp[-S_{ab}(t_a)] \\ &\quad - (r_D-2)r_D(x_1-1) \alpha_s(t_b) h_e(\alpha_e, \beta_b, b_2, b_1) S_f(x_1) \exp[-S_{ab}(t_b)] \}, \end{aligned} \quad (9)$$

where  $r_D = m_D/M_B$ ,  $r_b = m_b/M_B$ ;  $C_F = 4/3$  is a color factor;  $f_P$  is the decay constant of pseudoscalar meson (P). The factorization scales  $t_{a,b}$  are chosen as the maximal virtuality of internal particles in the hard amplitude, in order to suppress the higher-order corrections [29]. The functions  $h_e$  are displayed in Appendix B. The factor  $S_f(x)$  is the jet function from

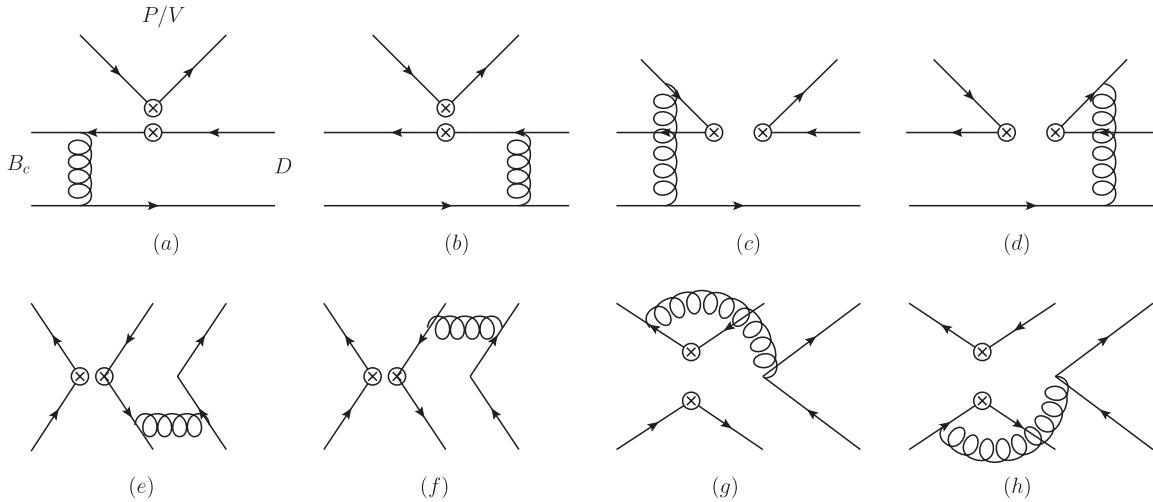


FIG. 1. The leading-order Feynman diagrams for the decays  $B_c \rightarrow D_{(s)}^{(*)}P, D_{(s)}^{(*)}V$ .

the threshold resummation, whose definitions can be found in Ref. [8]. The terms proportional to  $r_D^2$  have been neglected for small values. We can calculate the form factor from Eq. (9) if we take away the Wilson coefficients and  $f_P$ . For the  $(V - A)(V + A)$  operators, we have  $\mathcal{F}_e^{\text{LR}} = -\mathcal{F}_e^{\text{LL}}$  since only the axial-vector current contributes to the pseudoscalar meson production. For the  $(S - P)(S + P)$  operators, the formula is different:

$$\begin{aligned} \mathcal{F}_e^{\text{SP}} = & -4\sqrt{\frac{2}{3}}C_F f_B f_P \pi M_B^4 \int_0^1 dx_2 \int_0^\infty b_1 b_2 db_1 db_2 \phi_D(x_2, b_2) \{ [r_D(4r_b - x_2 - 1) \\ & - r_b + 2] \alpha_s(t_a) h_e(\alpha_e, \beta_a, b_1, b_2) S_t(x_2) \exp[-S_{ab}(t_a)] + [r_D(2 - 4x_1) \\ & + x_1] \alpha_s(t_b) h_e(\alpha_e, \beta_b, b_2, b_1) S_t(x_1) \exp[-S_{ab}(t_b)] \}. \end{aligned} \quad (10)$$

For the nonfactorizable emission diagrams (c) and (d), the decay amplitudes of three types of operators are

$$\begin{aligned} \mathcal{M}_e^{\text{LL}} = & \frac{8}{3} C_F f_B \pi M_B^4 \int_0^1 dx_2 dx_3 \int_0^\infty b_2 b_3 db_2 db_3 \phi_D(x_2, b_2) \phi_P^A(x_3) \{ [r_D(1 - x_1 - x_2) + x_1 + x_3 - 1] \\ & \times \alpha_s(t_c) h_e(\beta_c, \alpha_e, b_3, b_2) \exp[-S_{cd}(t_c)] - [r_D(1 - x_1 - x_2) \\ & + 2x_1 + x_2 - x_3 - 1] \alpha_s(t_d) h_e(\beta_d, \alpha_e, b_3, b_2) \exp[-S_{cd}(t_d)] \}, \end{aligned} \quad (11)$$

$$\begin{aligned} \mathcal{M}_e^{\text{LR}} = & \frac{8}{3} C_F f_B \pi M_B^4 r_P (1 + r_D) \int_0^1 dx_2 dx_3 \int_0^\infty b_2 b_3 db_2 db_3 \phi_D(x_2, b_2) \{ [(x_1 + x_3 - 1 + r_D(2x_1 + x_2 + x_3 - 2)) \phi_P^P(x_3) \\ & + (x_1 + x_3 - 1 + r_D(x_3 - x_2)) \phi_P^T(x_3)] \alpha_s(t_c) h_e(\beta_c, \alpha_e, b_3, b_2) \exp[-S_{cd}(t_c)] - [(x_1 - x_3 + r_D(2x_1 + x_2 - x_3 - 1)) \\ & \times \phi_P^P(x_3) + (x_3 - x_1 + r_D(x_3 + x_2 - 1)) \phi_P^T(x_3)] \alpha_s(t_d) h_e(\beta_d, \alpha_e, b_3, b_2) \exp[-S_{cd}(t_d)] \}, \end{aligned} \quad (12)$$

$$\begin{aligned} \mathcal{M}_e^{\text{SP}} = & \frac{8}{3} C_F f_B \pi M_B^4 \int_0^1 dx_2 dx_3 \int_0^\infty b_2 b_3 db_2 db_3 \phi_D(x_2, b_2) \phi_P^A(x_3) \{ [r_D(x_1 + x_2 - 1) \\ & - 2x_1 - x_2 - x_3 + 2] \alpha_s(t_c) h_e(\beta_c, \alpha_e, b_3, b_2) \exp[-S_{cd}(t_c)] \\ & - [x_3 - x_1 - r_D(1 - x_1 - x_2)] \alpha_s(t_d) h_e(\beta_d, \alpha_e, b_3, b_2) \exp[-S_{cd}(t_d)] \}, \end{aligned} \quad (13)$$

where  $r_P = m_0^P/M_B$ , with  $m_0^P$  as the chiral mass of the pseudoscalar meson.

For the factorizable emission diagrams (e) and (f), we keep the mass of the  $c$  quark in the  $D$  meson, while the mass of the light quark is neglected. The amplitudes are given as follows:

$$\begin{aligned} \mathcal{F}_a^{\text{LL}} = \mathcal{F}_a^{\text{LR}} = & -8C_F f_B \pi M_B^4 \int_0^1 dx_2 dx_3 \int_0^\infty b_2 b_3 db_2 db_3 \phi_D(x_2, b_2) \{ [\phi_P^A(x_3)(x_3 - 2r_D r_c) + r_P [\phi_P^P(x_3)(2r_D(x_3 + 1) - r_c) \\ & + \phi_P^T(x_3)(r_c + 2r_D(x_3 - 1))] \alpha_s(t_e) h_e(\alpha_a, \beta_e, b_2, b_3) \exp[-S_{ef}(t_e)] S_t(x_3) \\ & - [x_2 \phi_P^A(x_3) + 2r_P r_D(x_2 + 1) \phi_P^P(x_3)] \alpha_s(t_f) h_e(\alpha_a, \beta_f, b_3, b_2) \exp[-S_{ef}(t_f)] S_t(x_2) \}, \end{aligned} \quad (14)$$

$$\begin{aligned} \mathcal{F}_a^{\text{SP}} = & 16C_F f_B \pi M_B^4 \int_0^1 dx_2 dx_3 \int_0^\infty b_2 b_3 db_2 db_3 \phi_D(x_2, b_2) \{ [-\phi_P^A(x_3)(2r_D - r_c) \\ & + r_P [\phi_P^P(x_3)(4r_c r_D - x_3) + \phi_P^T(x_3)x_3] \alpha_s(t_e) h_e(\alpha_a, \beta_e, b_2, b_3) \exp[-S_{ef}(t_e)] S_t(x_3) \\ & - [x_2 r_D \phi_P^A(x_3) + 2r_P \phi_P^P(x_3)] \alpha_s(t_f) h_e(\alpha_a, \beta_f, b_3, b_2) \exp[-S_{ef}(t_f)] S_t(x_2) \}; \end{aligned} \quad (15)$$

and that of the nonfactorizable annihilation diagrams (g) and (h) are

$$\begin{aligned} \mathcal{M}_a^{\text{LL}} = & -\frac{8}{3} C_F f_B \pi M_B^4 \int_0^1 dx_2 dx_3 \int_0^\infty b_1 b_2 db_1 db_2 \phi_D(x_2, b_2) \{ [\phi_P^A(x_3)(r_c - x_1 + x_2) + r_P r_D [\phi_P^T(x_3)(x_2 - x_3) \\ & + \phi_P^P(x_3)(4r_c - 2x_1 + x_2 + x_3)] \alpha_s(t_g) h_e(\beta_g, \alpha_a, b_1, b_2) \exp[-S_{gh}(t_g)] + [-\phi_P^A(x_3)(r_b + x_1 + x_3 - 1) \\ & + r_P r_D [(x_2 - x_3) \phi_P^T(x_3) - \phi_P^P(x_3)(4r_b + 2x_1 + x_2 + x_3 - 2)] \alpha_s(t_h) h_e(\beta_h, \alpha_a, b_1, b_2) \exp[-S_{gh}(t_h)] \}, \end{aligned} \quad (16)$$

$$\begin{aligned} \mathcal{M}_a^{\text{LR}} = & \frac{8}{3} C_F f_B \pi M_B^4 \int_0^1 dx_2 dx_3 \int_0^\infty b_1 b_2 db_1 db_2 \phi_D(x_2, b_2) \{ [-\phi_P^A(x_3) r_D(r_c + x_1 - x_2) + r_P [-\phi_P^T(x_3)(-r_c - x_1 + x_3) \\ & + \phi_P^P(x_3)(r_c + x_1 - x_3)]] \alpha_s(t_g) h_e(\beta_g, \alpha_a, b_1, b_2) \exp[-S_{gh}(t_g)] + [-\phi_P^A(x_3) r_D(-r_b + x_1 + x_2 - 1) \\ & + r_P [(-r_b + x_1 + x_3 - 1)(\phi_P^P(x_3) + \phi_P^T(x_3))] \alpha_s(t_h) h_e(\beta_h, \alpha_a, b_1, b_2) \exp[-S_{gh}(t_h)] \}, \end{aligned} \quad (17)$$

$$\begin{aligned} \mathcal{M}_a^{\text{SP}} = & -\frac{8}{3} C_F f_B \pi M_B^4 \int_0^1 dx_2 dx_3 \int_0^\infty b_1 b_2 db_1 db_2 \phi_D(x_2, b_2) \{ [-\phi_P^A(x_3)(x_1 - x_3 - r_c) + r_P r_D [-\phi_P^T(x_3)(x_2 - x_3) \\ & + \phi_P^P(x_3)(4r_c - 2x_1 + x_2 + x_3)]] \alpha_s(t_g) h_e(\beta_g, \alpha_a, b_1, b_2) \exp[-S_{gh}(t_g)] + [-\phi_P^A(x_3)(r_b + x_1 + x_2 - 1) \\ & + r_P r_D [(-4r_b - 2x_1 - x_2 - x_3 + 2)\phi_P^P(x_3) - (x_2 - x_3)\phi_P^T(x_3)]] \alpha_s(t_h) h_e(\beta_h, \alpha_a, b_1, b_2) \exp[-S_{gh}(t_h)] \}. \end{aligned} \quad (18)$$

With the functions obtained in the above, the total decay amplitudes of 10 decay channels for the  $B_c \rightarrow D_{(s)}P$  can be given by

$$\begin{aligned} \mathcal{A}(B_c \rightarrow D^0 \pi^+) = & \xi_u [a_1 \mathcal{F}_e^{\text{LL}} + C_1 \mathcal{M}_e^{\text{LL}}] + \xi_c [a_1 \mathcal{F}_a^{\text{LL}} + C_1 \mathcal{M}_a^{\text{LL}}] - \xi_t [(C_3 + C_9)(\mathcal{M}_e^{\text{LL}} + \mathcal{M}_a^{\text{LL}}) \\ & + (C_5 + C_7)(\mathcal{M}_e^{\text{LR}} + \mathcal{M}_a^{\text{LR}}) + (C_4 + \frac{1}{3}C_3 + C_{10} + \frac{1}{3}C_9)(\mathcal{F}_a^{\text{LL}} + \mathcal{F}_e^{\text{LL}}) \\ & + (C_6 + \frac{1}{3}C_5 + C_8 + \frac{1}{3}C_7)(\mathcal{F}_a^{\text{SP}} + \mathcal{F}_e^{\text{SP}}], \end{aligned} \quad (19)$$

$$\begin{aligned} \sqrt{2} \mathcal{A}(B_c \rightarrow D^+ \pi^0) = & \xi_u [a_2 \mathcal{F}_e^{\text{LL}} + C_2 \mathcal{M}_e^{\text{LL}}] - \xi_c [a_1 \mathcal{F}_a^{\text{LL}} + C_1 \mathcal{M}_a^{\text{LL}}] - \xi_t \left[ \left( \frac{3}{2} C_{10} - C_3 + \frac{1}{2} C_9 \right) \mathcal{M}_e^{\text{LL}} \right. \\ & - (C_3 + C_9) \mathcal{M}_a^{\text{LL}} + \left( -C_5 + \frac{1}{2} C_7 \right) \mathcal{M}_e^{\text{LR}} + \left( -C_4 - \frac{1}{3} C_3 - C_{10} - \frac{1}{3} C_9 \right) \mathcal{F}_a^{\text{LL}} \\ & + \left( C_{10} + \frac{5}{3} C_9 - \frac{1}{3} C_3 - C_4 - \frac{3}{2} C_7 - \frac{1}{2} C_8 \right) \mathcal{F}_e^{\text{LL}} + \left( -C_6 - \frac{1}{3} C_5 + \frac{1}{2} C_8 + \frac{1}{6} C_7 \right) \mathcal{F}_e^{\text{SP}} \\ & \left. - (C_5 + C_7) \mathcal{M}_a^{\text{LR}} + \left( -C_6 - \frac{1}{3} C_5 - C_8 - \frac{1}{3} C_7 \right) \mathcal{F}_a^{\text{SP}} \right], \end{aligned} \quad (20)$$

$$\begin{aligned} \sqrt{2} \mathcal{A}(B_c \rightarrow D^+ \eta_q) = & \xi_u [a_2 \mathcal{F}_e^{\text{LL}} + C_2 \mathcal{M}_e^{\text{LL}}] + \xi_c [a_1 \mathcal{F}_a^{\text{LL}} + C_1 \mathcal{M}_a^{\text{LL}}] - \xi_t \left[ \left( 2C_4 + C_3 + \frac{1}{2} C_{10} - \frac{1}{2} C_9 \right) \mathcal{M}_e^{\text{LL}} \right. \\ & + (C_3 + C_9) \mathcal{M}_a^{\text{LL}} + \left( C_5 - \frac{1}{2} C_7 \right) \mathcal{M}_e^{\text{LR}} + (C_5 + C_7) \mathcal{M}_a^{\text{LR}} + \left( C_4 + \frac{1}{3} C_3 + C_{10} + \frac{1}{3} C_9 \right) \mathcal{F}_a^{\text{LL}} \\ & + \left( \frac{7}{3} C_3 + \frac{5}{3} C_4 + \frac{1}{3} (C_9 - C_{10}) \right) \mathcal{F}_e^{\text{LL}} + \left( 2C_5 + \frac{2}{3} C_6 + \frac{1}{2} C_7 + \frac{1}{6} C_8 \right) \mathcal{F}_e^{\text{LR}} \\ & \left. + \left( C_6 + \frac{1}{3} C_5 - \frac{1}{2} C_8 - \frac{1}{6} C_7 \right) \mathcal{F}_e^{\text{SP}} + \left( C_6 + \frac{1}{3} C_5 + C_8 + \frac{1}{3} C_7 \right) \mathcal{F}_a^{\text{SP}} \right], \end{aligned} \quad (21)$$

$$\begin{aligned} \mathcal{A}(B_c \rightarrow D^+ \eta_s) = & -\xi_t \left[ \left( C_4 - \frac{1}{2} C_{10} \right) \mathcal{M}_e^{\text{LL}} + \left( C_6 - \frac{1}{2} C_8 \right) \mathcal{M}_e^{\text{SP}} + \left( C_3 + \frac{1}{3} C_4 - \frac{1}{2} C_9 - \frac{1}{6} C_{10} \right) \mathcal{F}_e^{\text{LL}} \right. \\ & \left. + \left( C_5 + \frac{1}{3} C_6 - \frac{1}{2} C_7 - \frac{1}{6} C_8 \right) \mathcal{F}_e^{\text{LR}} \right], \end{aligned} \quad (22)$$

$$\begin{aligned} \sqrt{2} \mathcal{A}(B_c \rightarrow D_s^+ \eta_q) = & \xi_u [a_2 \mathcal{F}_e^{\text{LL}} + C_2 \mathcal{M}_e^{\text{LL}}] - \xi_t \left[ \left( 2C_4 + \frac{1}{2} C_{10} \right) \mathcal{M}_e^{\text{LL}} + \left( 2C_6 + \frac{1}{2} C_8 \right) \mathcal{M}_e^{\text{SP}} \right. \\ & \left. + \left( 2C_3 + \frac{2}{3} C_4 + \frac{1}{2} C_9 + \frac{1}{6} C_{10} \right) \mathcal{F}_e^{\text{LL}} + \left( 2C_5 + \frac{2}{3} C_6 + \frac{1}{2} C_7 + \frac{1}{6} C_8 \right) \mathcal{F}_e^{\text{LR}} \right], \end{aligned} \quad (23)$$

$$\begin{aligned}
\mathcal{A}(B_c \rightarrow D_s^+ \eta_s) = & \xi'_c [a_1 \mathcal{F}_a^{\text{LL}} + C_1 \mathcal{M}_a^{\text{LL}}] - \xi'_i \left[ \left( C_3 + C_4 - \frac{1}{2}(C_{10} + C_9) \right) \mathcal{M}_e^{\text{LL}} + (C_3 + C_9) \mathcal{M}_a^{\text{LL}} + \left( C_5 - \frac{1}{2} C_7 \right) \mathcal{M}_e^{\text{LR}} \right. \\
& + (C_5 + C_7) \mathcal{M}_a^{\text{LR}} + \left( C_4 + \frac{1}{3} C_3 + C_{10} + \frac{1}{3} C_9 \right) \mathcal{F}_a^{\text{LL}} + \left( C_6 - \frac{1}{2} C_8 \right) \mathcal{M}_e^{\text{SP}} + \frac{2}{3} (2(C_3 + C_4) \\
& - (C_9 + C_{10})) \mathcal{F}_e^{\text{LL}} + \left( C_5 + \frac{1}{3} C_6 - \frac{1}{2} C_7 - \frac{1}{6} C_8 \right) \mathcal{F}_e^{\text{LR}} + \left( C_6 + \frac{1}{3} C_5 - \frac{1}{2} C_8 - \frac{1}{6} C_7 \right) \mathcal{F}_e^{\text{SP}} \\
& \left. + \left( C_6 + \frac{1}{3} C_5 + C_8 + \frac{1}{3} C_7 \right) \mathcal{F}_a^{\text{SP}} \right], \tag{24}
\end{aligned}$$

$$\begin{aligned}
\mathcal{A}(B_c \rightarrow D_s^+ \bar{K}^0) = & \xi_c [a_1 \mathcal{F}_a^{\text{LL}} + C_1 \mathcal{M}_a^{\text{LL}}] - \xi_i \left[ \left( C_3 - \frac{1}{2} C_9 \right) \mathcal{M}_e^{\text{LL}} + (C_3 + C_9) \mathcal{M}_a^{\text{LL}} + \left( C_5 - \frac{1}{2} C_7 \right) \mathcal{M}_e^{\text{LR}} \right. \\
& + (C_5 + C_7) \mathcal{M}_a^{\text{LR}} + \left( C_4 + \frac{1}{3} C_3 + C_{10} + \frac{1}{3} C_9 \right) \mathcal{F}_a^{\text{LL}} + \left( C_4 + \frac{1}{3} C_3 - \frac{1}{2} C_{10} - \frac{1}{6} C_9 \right) \mathcal{F}_e^{\text{LL}} \\
& \left. + \left( C_6 + \frac{1}{3} C_5 - \frac{1}{2} C_8 - \frac{1}{6} C_7 \right) \mathcal{F}_e^{\text{SP}} + \left( C_6 + \frac{1}{3} C_5 + C_8 + \frac{1}{3} C_7 \right) \mathcal{F}_a^{\text{SP}} \right], \tag{25}
\end{aligned}$$

$$\mathcal{A}(B_c \rightarrow D_s^+ \pi^0) = \xi'_u [a_2 \mathcal{F}_e^{\text{LL}} + C_2 \mathcal{M}_e^{\text{LL}}] - \xi'_i \left[ \left( \frac{1}{2} (3C_9 + C_{10}) \mathcal{F}_e^{\text{LL}} + \frac{1}{2} (3C_7 + C_8) \right) \mathcal{F}_e^{\text{LR}} + \frac{3}{2} C_{10} \mathcal{M}_e^{\text{LL}} + \frac{3}{2} C_8 \mathcal{M}_e^{\text{SP}} \right], \tag{26}$$

with the CKM matrix element  $\xi_i = V_{id} V_{ib}^*$  and  $\xi'_i = V_{is} V_{ib}^*$  ( $i = u, c, t$ ). The combinations of Wilson coefficients are defined as  $a_1 = C_2 + C_1/3$  and  $a_2 = C_1 + C_2/3$ . The total decay amplitude of  $\mathcal{A}(B_c \rightarrow D^0 K^+)$  and  $\mathcal{A}(B_c \rightarrow D^+ K^0)$  can be obtained from Eqs. (19) and (25), respectively, with the following replacement:

$$\mathcal{A}(B_c \rightarrow D^0 K^+) = \mathcal{A}(B_c \rightarrow D^0 \pi^+) |_{\pi \rightarrow K, \xi_i \rightarrow \xi'_i}, \quad \mathcal{A}(B_c \rightarrow D^+ K^0) = \mathcal{A}(B_c \rightarrow D_s^+ \bar{K}^0) |_{D_s \rightarrow D, \xi_i \rightarrow \xi'_i}. \tag{27}$$

It should be noticed that, in Eqs. (21)–(24), the decay amplitudes are for the mixing basis of  $(\eta_q, \eta_s)$ . For the physical state  $(\eta, \eta')$ , the decay amplitudes are

$$\begin{aligned}
\mathcal{A}(B_c \rightarrow D^+ \eta) &= \mathcal{A}(B_c \rightarrow D^+ \eta_q) \cos \phi - \mathcal{A}(B_c \rightarrow D^+ \eta_s) \sin \phi, \\
\mathcal{A}(B_c \rightarrow D^+ \eta') &= \mathcal{A}(B_c \rightarrow D^+ \eta_q) \sin \phi + \mathcal{A}(B_c \rightarrow D^+ \eta_s) \cos \phi, \\
\mathcal{A}(B_c \rightarrow D_s^+ \eta) &= \mathcal{A}(B_c \rightarrow D_s^+ \eta_q) \cos \phi - \mathcal{A}(B_c \rightarrow D_s^+ \eta_s) \sin \phi, \\
\mathcal{A}(B_c \rightarrow D_s^+ \eta') &= \mathcal{A}(B_c \rightarrow D_s^+ \eta_q) \sin \phi + \mathcal{A}(B_c \rightarrow D_s^+ \eta_s) \cos \phi,
\end{aligned} \tag{28}$$

where  $\phi = 39.3^\circ$  is the mixing angle between the two states.

$$\begin{pmatrix} \eta \\ \eta' \end{pmatrix} = \begin{pmatrix} \cos \phi & -\sin \phi \\ \sin \phi & \cos \phi \end{pmatrix} \begin{pmatrix} \eta_q \\ \eta_s \end{pmatrix}. \tag{29}$$

### B. Amplitudes for $B_c \rightarrow D_{(s)} V$ decays

In  $B_c \rightarrow D_{(s)} V$  decays, the vector meson is longitudinally polarized. In the leading power contribution, the formula of each Feynman diagram for  $B_c \rightarrow D_{(s)} V$  is similar to that of the  $B_c \rightarrow D_{(s)} P$  modes, but with the replacements

$$\begin{aligned}
f_P \rightarrow f_V, \quad r_P \rightarrow r_V, \quad \phi_P^A \rightarrow \phi_V, \quad \phi_P^P \rightarrow -\phi_V^s, \\
\phi_P^T \rightarrow \phi_V^t.
\end{aligned} \tag{30}$$

The total decay amplitude for  $B_c \rightarrow D_{(s)} V$  can be obtained through the substitutions in Eqs. (19)–(27):

$$\pi \rightarrow \rho, \quad K \rightarrow K^*, \quad \eta_q \rightarrow \omega, \quad \eta_s \rightarrow \phi. \tag{31}$$

### C. Amplitudes for $B_c \rightarrow D_{(s)}^* V$ decays

The decay amplitude of  $B_c \rightarrow D_{(s)}^* V$  can be decomposed into

$$\begin{aligned}
\mathcal{A}(\epsilon_{D^*}, \epsilon_V) = & \mathcal{A}^L + \mathcal{A}^N \epsilon_{D^* T} \cdot \epsilon_{VT} \\
& + i \mathcal{A}^T \epsilon_{\alpha\beta\rho\sigma} n^\alpha v^\beta \epsilon_{D^* T}^\rho \epsilon_{VT}^\sigma,
\end{aligned} \tag{32}$$

where  $\epsilon_{D^* T}(\epsilon_{VT})$  is the transverse polarization vector for the  $D^*(V)$  meson.  $\mathcal{A}^L$  corresponds to the contributions of longitudinal polarization;  $\mathcal{A}^N$  and  $\mathcal{A}^T$  corresponds to the contributions of normal and transverse polarization, respectively. The factorization formulae for the longitudinal, normal, and transverse polarizations are all listed in Appendix A. There are also 10 channels for  $B_c \rightarrow D_{(s)}^* V$  decay modes. We can obtain the total decay amplitudes from those in  $B_c \rightarrow D_{(s)} V$  with replacing  $D_{(s)}$  by  $D_{(s)}^*$ .

### D. Amplitudes for $B_c \rightarrow D_{(s)}^{*}P$ decays

For  $B_c \rightarrow D_{(s)}^{*}P$ , only the longitudinal polarization of  $D_{(s)}^{*}$  will contribute. We can obtain their amplitudes from the longitudinal polarization amplitudes for the  $B_c \rightarrow D_{(s)}^{*}V$  decays with the following replacement in the distribution amplitudes:

$$\begin{aligned} f_V \rightarrow f_P, \quad r_V \rightarrow r_P, \quad \phi_V \rightarrow \phi_P^A, \quad \phi_V^s \rightarrow \phi_P^P, \\ \phi_V^t \rightarrow \phi_P^T. \end{aligned} \quad (33)$$

In fact, the  $B_c \rightarrow D_{(s)}^{*}P$  decay amplitudes are the same as the  $B_c \rightarrow D_{(s)}P$  ones only at leading power under the hierarchy  $M_{B_c} \gg m_{D^{(*)}} \gg \Lambda_{QCD}$ . An explicit derivation shows that the difference between the two kinds of channels occurs at  $\mathcal{O}(r_{D^{(*)}})$  and at the twist-3 level in Eqs. (9)–(18).

## III. NUMERICAL RESULTS AND DISCUSSIONS

The numerical results of our calculations depend on a set of input parameters. We list the decay constants of various mesons and parameters of hadronic wave functions in Table I. For the  $\eta - \eta'$  system, the decay constants  $f_q$  and  $f_s$  in the quark-flavor basis have been extracted from various related experiments [31,32]

$$f_q = (1.07 \pm 0.02)f_\pi, \quad f_s = (1.34 \pm 0.06)f_\pi. \quad (34)$$

For the CKM matrix elements, the quark masses, etc., we adopt the results from Ref. [33]:

$$\begin{aligned} |V_{ub}| &= (3.89 \pm 0.44) \times 10^{-3}, & |V_{ud}| &= 0.97425, \\ |V_{cb}| &= 0.0406, & |V_{cd}| &= 0.23, & |V_{us}| &= 0.2252, \\ |V_{cs}| &= 1.023, & \gamma &= (73_{-25}^{+22})^\circ, & m_c &= 1.27 \text{ GeV}, \\ m_b &= 4.2 \text{ GeV}, & m_\pi^0 &= 1.4 \text{ GeV}, \\ m_0^K &= 1.6 \text{ GeV}, & m_0^{\eta_q} &= 1.07 \text{ GeV}, \\ m_0^{\eta_s} &= 1.92 \text{ GeV}, & \Lambda_{QCD}^5 &= 0.112 \text{ GeV}. \end{aligned} \quad (35)$$

For the considered  $B_c \rightarrow D_{(s)}P$ ,  $B_c \rightarrow D_{(s)}^{*}P$ , and  $B_c \rightarrow D_{(s)}V$  decays, the branching ratios (BR) and the direct  $CP$  asymmetry  $A_{CP}^{\text{dir}}$  for a given mode can be written as

$$\text{BR} = \frac{G_F \tau_{B_c} (1 - r_D^2) |\mathcal{A}|^2}{32\pi M_B}, \quad A_{CP}^{\text{dir}} = \frac{|\bar{\mathcal{A}}|^2 - |\mathcal{A}|^2}{|\bar{\mathcal{A}}|^2 + |\mathcal{A}|^2}, \quad (36)$$

where the decay amplitudes  $\mathcal{A}$  have been given explicitly in Sec. II for each channel.  $\bar{\mathcal{A}}$  is the corresponding charge conjugate decay amplitude, which can be obtained by conjugating the CKM matrix elements in  $\mathcal{A}$ .

Our numerical results of  $CP$ -averaged branching ratios and direct  $CP$  asymmetries for  $B_c \rightarrow D_{(s)}P$  and  $B_c \rightarrow D_{(s)}V$  decays are listed in Tables II and III, respectively. The dominant topologies contributing to these decays are also indicated through the symbols  $T$  (color-allowed tree),  $C$  (color-suppressed tree),  $P$  (penguin), and  $A$  (annihilation). The first theoretical error in all our tables is referred to as the  $D_{(s)}$ -meson wave function: (1) The shape parameter  $\omega_D = 0.60 \pm 0.05$  for the  $D/D^*$  meson and  $\omega_{D_s} = 0.80 \pm 0.05$  for the  $D_s/D_s^*$  meson; (2) The decay constant  $f_D = (206.7 \pm 8.9)$  MeV for the  $D$  meson and  $f_{D_s} = (257.5 \pm 6.1)$  MeV for the  $D_s$  meson. The second error is from the combined uncertainty in the CKM matrix elements  $V_{ub}$  and the angle of unitarity triangle  $\gamma$ , which are given in Eq. (35). The third error arises from the hard scale  $t$  varying from  $0.75t$  to  $1.25t$ , which characterizes the size of next-to-leading-order QCD contributions. Most of the branching ratios are sensitive to the hadronic parameters and the CKM matrix elements. The  $CP$  asymmetry parameter is only sensitive to the next-to-leading-order contributions, since the uncertainty of hadronic parameters is mostly canceled by the ratios.

We also cite theoretical results for the relevant decays evaluated in the LFQM model [3] and the RCQM model [5] to make a comparison in Tables II and III. Our pQCD results are generally close to RCQM results but differ substantially from the ones obtained by LFQM. This is

TABLE I. The decay constants and the hadronic meson wave function parameters taken from the light-cone sum rules [30].

		The decay constants (MeV)										
$f_{B_c}$	$f_D$	$f_{D_s}$	$f_\pi$	$f_K$	$f_\rho$	$f_\rho^T$	$f_\omega$	$f_\omega^T$	$f_\phi$	$f_\phi^T$	$f_{K^*}$	$f_{K^*}^T$
489	$206.7 \pm 8.9$	$257.5 \pm 6.1$	131	160	209	165	195	145	231	200	217	185
		Values of Gegenbauer moments										
		$\pi$	$K$	$\eta_q$	$\eta_s$							
$a_1^P$	$\dots$	$\dots$	0.17	$\dots$	$\dots$							
$a_2^P$	0.25	0.115	0.115	0.115	0.115							
$a_4^P$	-0.015	-0.015	-0.015	-0.015	-0.015							
		$\rho$	$\omega$	$\phi$	$K^*$							
$a_1^\parallel$	$\dots$	$\dots$	$\dots$	$\dots$	0.03							
$a_2^\parallel$	0.15	0.15	0.15	0.18	0.11							
$a_1^\perp$	$\dots$	$\dots$	$\dots$	$\dots$	0.04							
$a_2^\perp$	0.14	0.14	0.14	0.14	0.10							

TABLE II.  $CP$ -averaged branching ratios and direct  $CP$  asymmetries for  $B_c \rightarrow D_{(s)}P$  decays, together with results from RCQM and LFQM.

channels	Class	$\mathcal{BR}(10^{-7})$			$A_{CP}^{\text{dir}}(\%)$	
		This work	RCQM <sup>a</sup>	LFQM	This work	RCQM
$B_c \rightarrow D^0 \pi^+$	T	$26.7^{+3.1+6.0+0.8}_{-3.5-5.6-0.6}$	22.9	4.3	$-41.2^{+4.5+11.1+0.8}_{-4.6-7.8-1.2}$	6.5
$B_c \rightarrow D^+ \pi^0$	C,A	$0.82^{+0.24+0.55+0.06}_{-0.16-0.41-0.01}$	2.1	0.067	$2.3^{+6.3+1.4+15.0}_{-3.0-0.8-18.8}$	-1.9
$B_c \rightarrow D^0 K^+$	A,P	$47.8^{+17.2+2.2+5.4}_{-9.1-1.7-3.6}$	44.5	0.35	$-34.8^{+4.9+7.4+1.8}_{-2.6-3.7-1.3}$	-4.6
$B_c \rightarrow D^+ K^0$	A,P	$46.9^{+15.6+0.3+7.4}_{-12.3-0.3-4.6}$	49.3	...	$2.3^{+0.4+0.9+0.0}_{-0.2-0.5-0.0}$	-0.8
$B_c \rightarrow D^+ \eta$	C,A	$0.92^{+0.15+0.21+0.03}_{-0.15-0.25-0.00}$	...	0.087	$40.8^{+0.0+18.4+15.6}_{-2.9-14.0-13.5}$	...
$B_c \rightarrow D^+ \eta'$	C,A	$0.91^{+0.12+0.16+0.06}_{-0.10-0.20-0.03}$	...	0.048	$-14.0^{+0.6+4.6+15.9}_{-1.5-5.2-11.9}$	...
$B_c \rightarrow D_s^+ \pi^0$	C,P	$0.41^{+0.04+0.01+0.02}_{-0.04-0.02-0.02}$	...	0.0067	$46.7^{+1.4+6.3+2.5}_{-1.4-11.8-2.8}$	...
$B_c \rightarrow D_s^+ \bar{K}^0$	A,P	$2.1^{+0.9+0.3+0.3}_{-0.6-0.3-0.2}$	1.9	...	$54.3^{+6.9+5.3+0.0}_{-7.2-8.0-0.3}$	13.3
$B_c \rightarrow D_s^+ \eta$	A,P	$17.3^{+1.7+0.5+3.3}_{-1.8-0.6-1.2}$	...	0.009	$2.8^{+0.0+0.4+1.1}_{-0.1-0.7-1.2}$	...
$B_c \rightarrow D_s^+ \eta'$	A,P	$51.0^{+4.9+0.4+6.7}_{-5.4-0.3-3.5}$	...	0.0048	$1.1^{+0.1+0.2+0.7}_{-0.0-0.2-0.6}$	...

<sup>a</sup>We use the results of decay widths in Ref. [5], but we take  $\tau_{B_c} = 0.453$  ps to estimate the branching ratio.

 TABLE III.  $CP$ -averaged branching ratios and direct  $CP$  asymmetries for  $B_c \rightarrow D_{(s)}V$  decays, together with results from RCQM and LFQM.

channels	Class	$\mathcal{BR}(10^{-7})$			$A_{CP}^{\text{dir}}(\%)$	
		This work	RCQM	LFQM	This work	RCQM
$B_c \rightarrow D^0 \rho^+$	T	$66.2^{+7.6+16.0+1.6}_{-7.6-14.1-1.3}$	60.0	13	$-24.5^{+2.6+5.3+0.3}_{-0.4-3.2-0.8}$	3.8
$B_c \rightarrow D^+ \rho^0$	C,A	$1.4^{+0.1+0.5+0.1}_{-0.2-0.5-0.2}$	3.9	0.2	$79.8^{+0.3+11.2+3.4}_{-5.8-19.6-10.7}$	-3.0
$B_c \rightarrow D^0 K^{*+}$	A,P	$25.9^{+2.7+0.9+1.5}_{-3.0-0.8-0.8}$	34.7	0.68	$-66.2^{+1.8+15.1+0.7}_{-0.6-6.5-0.0}$	-6.2
$B_c \rightarrow D^+ K^{*0}$	A,P	$19.1^{+3.3+0.1+0.7}_{-2.5-0.0-0.7}$	28.8	...	$3.5^{+0.0+0.5+0.5}_{-0.1-0.8-0.3}$	-0.8
$B_c \rightarrow D^+ \omega$	C,A	$1.9^{+0.3+0.5+0.0}_{-0.3-0.6-0.0}$	...	0.15	$-3.6^{+3.9+1.3+13.4}_{-1.2-1.6-10.7}$	...
$B_c \rightarrow D^+ \phi$	P	$0.008^{+0.001+0.0+0.001}_{-0.001-0.0-0.001}$	...	...	...	...
$B_c \rightarrow D_s^+ \rho^0$	C,P	$0.95^{+0.10+0.02+0.04}_{-0.09-0.01-0.04}$	...	...	$50.2^{+1.0+5.9+2.5}_{-1.1-11.9-3.2}$	...
$B_c \rightarrow D_s^+ \bar{K}^{*0}$	A,P	$1.4^{+0.2+0.0+0.1}_{-0.2-0.1-0.1}$	1.0	...	$61.0^{+0.0+6.5+4.5}_{-0.3-14.2-3.6}$	13.3
$B_c \rightarrow D_s^+ \omega$	C,P	$0.31^{+0.03+0.07+0.07}_{-0.03-0.07-0.05}$	...	0.016	$44.9^{+0.8+17.1+10.3}_{-1.6-14.9-13.6}$	...
$B_c \rightarrow D_s^+ \phi$	A,P	$27.0^{+4.8+0.1+2.0}_{-1.2-0.0-0.4}$	15.7	0.0048	$3.3^{+0.0+0.4+0.3}_{-0.3-0.8-0.4}$	-0.8

due to the fact that LFQM used smaller form factors  $F^{B_c \rightarrow D}(q^2 = 0) = 0.086$  at maximum recoil, which is quite smaller than other model predictions [4] and also another covariant LFQM results [34]. In fact, these model calculations all give consistent form factors at the zero-coil region, considering only soft contributions by the overlap between the initial and final-state meson wave functions, which is good at the zero-recoil region. At the maximum-recoil region, which is the case for nonleptonic  $B$  decays, the soft contribution is suppressed, since a hard gluon is needed, as discussed in the previous section. Furthermore, LFQM only considers the contribution of current-current operators at the tree level; therefore, they cannot give predictions for those modes without tree diagram contributions like  $B_c \rightarrow D^+ K^0$  and  $B_c \rightarrow D_s^+ \bar{K}^0$ . For the color-suppressed decays

(C), our predictions differ from the ones of RCQM, since in these modes, the contributions from the nonfactorizable emission diagram and annihilation diagram dominated the branching ratio, which are not calculable in RCQM.

Our numerical results of the  $CP$ -averaged branching ratios and direct  $CP$  asymmetries for  $B_c \rightarrow D_{(s)}^* P$  decays are listed in Table IV, together with the RCQM model predictions. Again, our results are similar with the RCQM model for the tree dominant mode (T). But for the annihilation dominant and penguin dominant modes (A,P), the branching ratios obtained in the RCQM are one order of magnitude smaller than ours. The reason is that these decay amplitudes are governed by the QCD penguin parameters  $a_4$  and  $a_6$  in the combination  $a_4 + Ra_6$  [35] in the factorization hypothesis. The coefficient  $R$  arises from

TABLE IV.  $CP$ -averaged branching ratios and direct  $I$  asymmetries for  $B_c \rightarrow D_{(s)}^{(*)}P$  decays, together with results from RCQM.

channels	Class	$\mathcal{BR}(10^{-7})$		$A_{CP}^{\text{dir}}(\%)$	
		This work	RCQM	This work	RCQM
$B_c \rightarrow D^{*0}\pi^+$	T	$18.8^{+2.0+4.1+0.4}_{-2.0-3.5-0.5}$	19.6	$64.0^{+12.0+6.1+0.7}_{-7.6-13.0-0.5}$	1.5
$B_c \rightarrow D^{*+}\pi^0$	C,A	$1.3^{+0.4+0.2+0.0}_{-0.3-0.3-0.0}$	0.66	$9.6^{+3.3+3.4+10.8}_{-2.7-3.3-8.8}$	-2.1
$B_c \rightarrow D^{*0}K^+$	A,P	$73.5^{+31.0+0.8+0.7}_{-23.4-1.1-0.4}$	4.9	$25.0^{+4.4+3.2+0.1}_{-4.1-6.1-0.3}$	-8.2
$B_c \rightarrow D^{*+}K^0$	A,P	$77.8^{+25.4+0.2+7.2}_{-24.0-0.2-5.2}$	2.8	$-0.3^{+0.0+0.0+0.0}_{-0.0-0.0-0.0}$	-8.2
$B_c \rightarrow D^{*+}\eta$	C,A	$0.34^{+0.14+0.19+0.04}_{-0.09-0.15-0.00}$	...	$-2.0^{+0.0+0.7+22.8}_{-2.4-1.5-30.0}$	...
$B_c \rightarrow D^{*+}\eta'$	C,A	$0.15^{+0.08+0.08+0.03}_{-0.05-0.06-0.01}$	...	$-41.8^{+17.5+13.0+24.3}_{-24.5-13.0-19.2}$	...
$B_c \rightarrow D_s^{*+}\pi^0$	C,P	$0.27^{+0.02+0.03+0.01}_{-0.04-0.02-0.02}$	...	$29.9^{+2.4+5.3+1.8}_{-1.9-8.2-1.5}$	...
$B_c \rightarrow D_s^{*+}\bar{K}^0$	A,P	$1.6^{+0.2+0.1+0.2}_{-0.3-0.1-0.1}$	0.21	$-3.3^{+0.4+0.6+0.9}_{-1.0-0.4-0.4}$	13.3
$B_c \rightarrow D_s^{*+}\eta$	A,P	$16.7^{+5.3+0.3+0.1}_{-4.0-0.2-0.3}$	...	$-0.7^{+0.2+0.2+0.6}_{-0.2-0.0-0.3}$	...
$B_c \rightarrow D_s^{*+}\eta'$	A,P	$14.4^{+6.6+0.1+0.5}_{-4.6-0.1-0.6}$	...	$0.02^{+0.01+0.00+0.55}_{-0.02-0.01-0.52}$	...

the penguin operator  $O_6$ , where  $R > 0$  for  $B \rightarrow PP$ ,  $R = 0$  for  $PV$  and  $VV$  final states, and  $R < 0$  for  $B \rightarrow VP$ ; the second meson in the final states is the one emitted from vacuum. Therefore, the branching ratios of various types of decays have the following pattern in the factorization approach:

$$\begin{aligned} \text{BR}(B_c \rightarrow DP) &> \text{BR}(B_c \rightarrow DV) \\ &\sim \text{BR}(B_c \rightarrow D^*V) > \text{BR}(B_c \rightarrow D^*P), \end{aligned} \quad (37)$$

as a consequence of the interference between the  $a_4$  and  $a_6$  penguin terms. In the contrary, we have additional nonfactorization contributions and large annihilation-type contributions in the pQCD approach, which spoils the relation in Eq. (37).

As expected, the annihilation-type diagrams give large contributions in the  $B_c$ -meson decays, because the annihilation-type diagram contributions are enhanced by the CKM factor  $V_{cb}^*V_{cq}$  [7,36]. For the  $b \rightarrow d$  process,  $|\frac{V_{cb}^*V_{cd}}{V_{ub}^*V_{ud}}| = 2.5$ ; for the  $b \rightarrow s$  process,  $|\frac{V_{cb}^*V_{cs}}{V_{ub}^*V_{us}}| = 47$ . The annihilation diagram contributions are the dominant contribution in some  $b \rightarrow s$  processes. Therefore, we have the ratio relation  $\frac{\text{BR}(B_c \rightarrow D^{(*)0}K^{(*)+})}{\text{BR}(B_c \rightarrow D^{(*)+}K^{(*)0})} \approx 1$  for these two annihilation-dominant  $b \rightarrow s$  transition processes.

For the color-suppressed decays, our predictions differ from the ones of RCQM, since in these modes, the contributions from the nonfactorizable emission diagram and annihilation diagram dominated the branching ratio, which are not calculable in RCQM. For example, in decays  $B_c \rightarrow D^{(*)+}(\pi^0, \eta, \eta', \rho^0, \omega)$ , the nonfactorizable contribution, which is proportional to the large Wilson coefficient  $C_2$ , is the dominant contribution. In fact, the annihilation diagrams can also give relatively large contributions for the enhancement by CKM factor. We also find that the twist-3 distribution amplitudes play an important role, especially in the factorizable annihilation

diagrams. As stated in Sec. II D, the  $B_c \rightarrow DP(V)$  decay amplitudes are different from  $B_c \rightarrow D^*P(V)$  ones only at twist-3 level. The numerical results show that the contributions from factorizable annihilation diagrams have an opposite sign between the two types of channels. For example, this results in a constructive interference between nonfactorizable emission diagrams and factorizable annihilation diagrams for  $B_c \rightarrow D^{*+}\pi^0$ , but a destructive interference for  $B_c \rightarrow D^+\pi^0$ . This makes  $\text{BR}(B_c \rightarrow D^{*+}\pi^0)$  larger than  $\text{BR}(B_c \rightarrow D^+\pi^0)$ . Similarly, we have  $\text{BR}(B_c \rightarrow D^{*+}\rho^0) > \text{BR}(B_c \rightarrow D^+\rho^0)$ . However, for  $B_c \rightarrow D^{(*)+}\eta(\eta')$ , while the  $d\bar{d}$  part contributes to the annihilation diagrams, the constructive or destructive interference situation are just the reverse, and  $\text{BR}(B_c \rightarrow D^{*+}\eta(\eta'))$  are smaller than  $\text{BR}(B_c \rightarrow D^+\eta(\eta'))$ .

For another kind of  $b \rightarrow s$  processes, the decays  $B_c \rightarrow D_s^{(*)+}(\pi^0, \rho^0, \omega)$  have a small branching ratio at  $\mathcal{O}(10^{-8})$  due to the absent annihilation diagram contributions, and the emission diagram contributions suppressed by CKM matrix elements  $|V_{ub}^*V_{us}|$ . Since the contribution of the penguin operator is comparable to the one of the tree operator, the interference between the two contributions is large. As a result, a big  $CP$  asymmetry is predicted in these decays. The branching ratio is even smaller  $\sim 10^{-10}$ , and there is no  $CP$  violation for  $B_c \rightarrow D^{(*)+}\phi$  decays, since there are only penguin-diagram contributions. All these and other rare decays are also important, since they are quite sensitive to new-physics contributions.

For the  $B_c \rightarrow D_{(s)}^{(*)}V$  decays, the branching ratios and the transverse polarization fractions  $\mathcal{R}_T$  are given as

$$\begin{aligned} \text{BR} &= \frac{G_F \tau_{B_c}}{32\pi M_B} (1 - r_D^2) \sum_{i=0,+,-} |\mathcal{A}_i|^2, \\ \mathcal{R}_T &= \frac{|\mathcal{A}_+|^2 + |\mathcal{A}_-|^2}{|\mathcal{A}_0|^2 + |\mathcal{A}_+|^2 + |\mathcal{A}_-|^2}, \end{aligned} \quad (38)$$

TABLE V.  $CP$ -averaged branching ratios, direct  $CP$  asymmetries, and the transverse polarizations fractions for  $B_c \rightarrow D_{(s)}^* V$  decays, together with results from RCQM.

channels	Class	$BR(10^{-7})$		$A_{CP}^{\text{dir}}(\%)$		$\mathcal{R}_T(\%)$	
		This work	RCQM	This work	RCQM	This work	
$B_c \rightarrow D^{*0} \rho^+$	T	$55.3^{+8.6+11.9+1.5}_{-5.0-11.1-1.4}$	59.7	$-24.1^{+3.0+4.2+0.4}_{-3.4-2.7-0.4}$	3.8	$16.4^{+2.5+2.0+0.3}_{-1.7-1.4-0.1}$	
$B_c \rightarrow D^{*+} \rho^0$	C,A	$3.8^{+1.0+0.5+0.1}_{-0.8-0.6-0.1}$	13.0	$30.2^{+0.0+2.6+5.4}_{-1.5-5.8-7.6}$	-3.0	$54.3^{+1.8+4.0+0.5}_{-0.9-2.4-0.4}$	
$B_c \rightarrow D^{*0} K^{*+}$	A,P	$161^{+59+5+11}_{-40-4-9}$	37.7	$-14.9^{+1.1+3.1+0.3}_{-0.8-1.7-0.1}$	-6.2	$52.6^{+1.5+2.3+1.3}_{-1.1-1.8-0.7}$	
$B_c \rightarrow D^{*+} K^{*0}$	A,P	$172^{+57+1+11}_{-42-1-9}$	30.6	$0.4^{+0.0+0.0+0.0}_{-0.0-0.1-0.0}$	-0.8	$57.4^{+0.6+0.1+0.9}_{-0.7-0.1-0.4}$	
$B_c \rightarrow D^{*+} \omega$	C,A	$2.4^{+0.4+0.9+0.2}_{-0.6-0.7-0.1}$	...	$-7.8^{+1.0+2.6+5.8}_{-0.0-3.4-5.0}$	...	$56.0^{+1.2+9.6+0.7}_{-0.5-6.5-0.7}$	
$B_c \rightarrow D^{*+} \phi$	P	$0.004^{+0.001+0+0}_{-0-0-0.001}$	...	...	...	$11.4^{+22.3+0.0+5.3}_{-5.4-0.0-6.9}$	
$B_c \rightarrow D_s^{*+} \rho^0$	C,P	$0.72^{+0.08+0.03+0.02}_{-0.08-0.03-0.03}$	...	$-29.3^{+1.3+7.6+1.4}_{-1.1-4.5-0.9}$	-3.0	$11.2^{+0.5+2.1+0.2}_{-0.3-1.4-0.1}$	
$B_c \rightarrow D_s^{*+} \bar{K}^{*0}$	A,P	$4.3^{+1.3+0.4+0.3}_{-1.0-0.3-0.2}$	2.9	$6.2^{+0.1+1.3+0.0}_{-0.3-1.8-0.1}$	13.3	$68.8^{+2.1+3.9+0.8}_{-2.3-4.4-0.4}$	
$B_c \rightarrow D_s^{*+} \omega$	C,P	$0.26^{+0.03+0.04+0.07}_{-0.01-0.05-0.04}$	...	$-21.3^{+5.3+6.8+7.9}_{-4.6-6.8-4.7}$	...	$49.5^{+8.8+2.1+4.4}_{-10.9-1.2-2.8}$	
$B_c \rightarrow D_s^{*+} \phi$	A,P	$137.3^{+39.3+0.5+10.5}_{-27.8-0.5-7.5}$	38.8	$0.3^{+0.1+0.1+0.0}_{-0.1-0.1-0.0}$	-0.8	$67.5^{+2.1+0.1+1.4}_{-3.1-0.2-1.5}$	

where the helicity amplitudes  $\mathcal{A}_i$  have the following relationships with  $\mathcal{A}^{L,N,T}$ :

$$\mathcal{A}_0 = \mathcal{A}^L, \quad \mathcal{A}_{\pm} = \mathcal{A}^N \pm \mathcal{A}^T. \quad (39)$$

Our numerical results of the  $CP$ -averaged branching ratios, direct  $CP$  asymmetries, and the transverse polarization fractions for  $B_c \rightarrow D_{(s)}^* V$  decays are shown in Table V. The transverse polarization contributions are usually suppressed by the factor  $r_V$  or  $r_{D^*}$  comparing with the longitudinal polarization contributions; thus, we do have relatively small transverse polarization fractions for the tree-dominant decay ( $\mathcal{R}_T(B_c \rightarrow D^{*0} \rho^+) = 16.4\%$ ) and the pure penguin type decay ( $\mathcal{R}_T(B_c \rightarrow D^{*+} \phi) = 11.5\%$ ). For the pure-emission-type decay  $B_c \rightarrow D_s^{*+} \omega$ , the transverse polarization fraction is large because the nonfactorizable emission diagram induced by operate  $O_6$  can enhance the transverse polarization sizably. The fact that the nonfactorizable contribution can give large transverse polarization contribution is also observed in the  $B^0 \rightarrow \rho^0 \rho^0$ ,  $\omega \omega$  decays [37]. For other decays, the annihilation-type contributions dominate the branching ratios due to the large Wilson coefficients. Therefore, the transverse polarizations take a larger ratio in the branching ratios, which can reach 50% ~ 70%. This is similar to the case of  $B \rightarrow \phi K^*$  and various  $B \rightarrow \rho K^*$  decays [38,39].

From Table V, one can also see that our branching ratios for  $B_c \rightarrow D^{*+} K^{*0}$ ,  $D^{*0} K^{*+}$ ,  $D_s^{*+} \bar{K}^{*0}$ ,  $D_s^{*+} \phi$  decays, are about 2 to 5 times larger than those in the RCQM model, due to the sizable contributions of transverse polarization amplitudes. Another point should be addressed that the annihilation contributions with a strong phase have remarkable effects on the direct  $CP$  asymmetries in these decays. As a result, our predictions are somewhat larger than those from RCQM.

## IV. CONCLUSION

In this paper, we investigate the two body nonleptonic decays of the  $B_c$  meson with the final states involving one  $D_{(s)}^{(*)}$  meson in the pQCD approach based on  $k_T$  factorization. It is found that the nonfactorizable emission and annihilation-type diagrams are possible to give a large contribution, especially for those color-suppressed modes and annihilation-diagram-dominant modes. All the branching ratios and  $CP$  asymmetry parameters are calculated, and the ratios of the transverse polarization contributions in the  $B_c \rightarrow D_{(s)}^* V$  decays are estimated. Because of the different weak phase and strong phase from tree diagrams, penguin diagrams, and annihilation diagrams, we predict a possible large direct  $CP$  violation in some channels. We also find that the transverse polarization contributions in some channels, which mainly come from the nonfactorizable emission diagrams or annihilation-type diagrams, are large.

Generally, our predictions for the branching ratios in the tree-dominant  $B_c$  decays are in good agreements with that of the RCQM model. But we have much larger branching ratios in the color-suppressed, annihilation-diagram-dominant  $B_c$  decays, due to the included nonfactorizable diagram and annihilation-type diagram contributions.

## ACKNOWLEDGMENTS

We thank Hsiang-nan Li and Fusheng Yu for helpful discussions. This work is partially supported by National Natural Science Foundation of China under the Grants No. 10735080, and No. 11075168; Natural Science Foundation of Zhejiang Province of China, Grant No. Y606252 and Scientific Research Fund of Zhejiang Provincial Education Department of China, Grant No. 20051357.

**APPENDIX A: FACTORIZATION FORMULAS FOR  $B_c \rightarrow D^*V$** 

We mark L, N and T to denote the contributions from longitudinal polarization, normal polarization, and transverse polarization, respectively.

$$\begin{aligned} \mathcal{F}_e^{\text{LLL}} &= 2\sqrt{\frac{2}{3}}\pi C_f f_B f_V M_B^4 \int_0^1 dx_2 \int_0^\infty b_1 b_2 db_1 db_2 \phi_{D^{(*)}}^*(x_2, b_2) \\ &\quad \times \{[x_2 - 2r_b + r_D(r_b - 2x_2)]\alpha_s(t_a)h_e(\alpha_e, \beta_a, b_1, b_2)S_t(x_2) \\ &\quad \times \exp[-S_{ab}(t_a)] + [r_D^2(x_1 - 1)]\alpha_s(t_b)h_e(\alpha_e, \beta_b, b_2, b_1)S_t(x_1) \exp[-S_{ab}(t_b)]\}, \end{aligned} \quad (\text{A1})$$

$$\begin{aligned} \mathcal{F}_e^{\text{LLN}} &= 2\sqrt{\frac{2}{3}}\pi C_f f_B f_V M_B^4 r_V \int_0^1 dx_2 \int_0^\infty b_1 b_2 db_1 db_2 \phi_{D^{(*)}}^*(x_2, b_2) \\ &\quad \times \{[r_b - 2 + r_D(x_2 + 1 - 4r_b)]\alpha_s(t_a)h_e(\alpha_e, \beta_a, b_1, b_2)S_t(x_2) \\ &\quad \times \exp[-S_{ab}(t_a) + r_D[2x_1 - 1]\alpha_s(t_b)h_e(\alpha_e, \beta_b, b_2, b_1)S_t(x_1) \exp[-S_{ab}(t_b)]\}, \end{aligned} \quad (\text{A2})$$

$$\begin{aligned} \mathcal{F}_e^{\text{LLT}} &= 2\sqrt{\frac{2}{3}}\pi C_f f_B f_V M_B^4 r_V \int_0^1 dx_2 \int_0^\infty b_1 b_2 db_1 db_2 \phi_{D^{(*)}}^*(x_2, b_2) \\ &\quad \times \{[r_b - 2 + r_D(1 - x_2)]\alpha_s(t_a)h_e(\alpha_e, \beta_a, b_1, b_2)S_t(x_2) \\ &\quad \times \exp[-S_{ab}(t_a)] - r_D\alpha_s(t_b)h_e(\alpha_e, \beta_b, b_2, b_1)S_t(x_1) \exp[-S_{ab}(t_b)]\}, \end{aligned} \quad (\text{A3})$$

$$\mathcal{F}_e^{\text{LRL}} = \mathcal{F}_e^{\text{LLL}}, \quad \mathcal{F}_e^{\text{LRN}} = \mathcal{F}_e^{\text{LLN}}, \quad \mathcal{F}_e^{\text{LRT}} = \mathcal{F}_e^{\text{LLT}}. \quad (\text{A4})$$

The factorizable emission topology contribution  $\mathcal{F}_e^{\text{SP},i} (i = L, N, T)$  vanishes due to the conservation of charge parity.

$$\begin{aligned} \mathcal{M}_e^{\text{LLL}} &= -\frac{8}{3}\pi C_f f_B M_B^4 \int_0^1 dx_2 dx_3 \int_0^\infty b_2 b_3 db_2 db_3 \phi_{D^{(*)}}^*(x_2, b_2) \phi_V(x_3) \\ &\quad \times \{[1 - x_1 - x_3 - r_D(x_1 + x_2 - 1)]\alpha_s(t_c)h_e(\beta_c, \alpha_e, b_3, b_2) \exp[-S_{cd}(t_c)] \\ &\quad + [-1 + 2x_1 + x_2 - x_3 - r_D(x_1 + x_2 - 1)]\alpha_s(t_d)h_e(\beta_d, \alpha_e, b_3, b_2) \exp[-S_{cd}(t_d)]\}, \end{aligned} \quad (\text{A5})$$

$$\begin{aligned} \mathcal{M}_e^{\text{LLN}} &= \frac{8}{3}\pi C_f f_B M_B^4 r_V \int_0^1 dx_2 dx_3 \int_0^\infty b_2 b_3 db_2 db_3 \phi_{D^{(*)}}^*(x_2, b_2) \{[(x_1 + x_3 - 1)\phi_V^v(x_3) + 2r_D(x_3 - x_2) \\ &\quad \times \phi_V^a(x_3)]\alpha_s(t_c)h_e(\beta_c, \alpha_e, b_3, b_2) \exp[-S_{cd}(t_c)] - [(-2r_D(1 - 2x_1 - x_2 + x_3) - x_1 + x_3)\phi_V^v(x_3) \\ &\quad + 2(r_D(1 - x_2 - x_3) - 2x_1 + 2x_3)\phi_V^a(x_3)]\alpha_s(t_d)h_e(\beta_d, \alpha_e, b_3, b_2) \exp[-S_{cd}(t_d)]\}, \end{aligned} \quad (\text{A6})$$

$$\begin{aligned} \mathcal{M}_e^{\text{LLT}} &= \frac{8}{3}\pi C_f f_B M_B^4 r_V \int_0^1 dx_2 dx_3 \int_0^\infty b_2 b_3 db_2 db_3 \phi_{D^{(*)}}^*(x_2, b_2) \{[(x_1 + x_3 - 1)\phi_V^v(x_3) - 2r_D(2x_1 + x_2 + x_3 - 2) \\ &\quad \times \phi_V^a(x_3)]\alpha_s(t_c)h_e(\beta_c, \alpha_e, b_3, b_2) \exp[-S_{cd}(t_c)] - [(x_3 - x_1)\phi_V^v(x_3) \\ &\quad + 2(r_D(2x_1 + x_2 - x_3 - 1) - 2x_1 + 2x_3)\phi_V^a(x_3)]\alpha_s(t_d)h_e(\beta_d, \alpha_e, b_3, b_2) \exp[-S_{cd}(t_d)]\}, \end{aligned} \quad (\text{A7})$$

$$\begin{aligned} \mathcal{M}_e^{\text{LRL}} &= -\frac{8}{3}\pi C_f f_B M_B^4 \int_0^1 dx_2 dx_3 \int_0^\infty b_2 b_3 db_2 db_3 \phi_{D^{(*)}}^*(x_2, b_2) \phi_V(x_3) \\ &\quad \times \{[(x_1 + x_3 - 1 + r_D(x_2 - x_3))\phi_V^s(x_3) + (x_1 + x_3 - 1 - r_D(2x_1 + x_2 + x_3 - 2)) \\ &\quad \times \phi_V^t(x_3)]\alpha_s(t_c)h_e(\beta_c, \alpha_e, b_3, b_2) \exp[-S_{cd}(t_c)] - [(x_1 - x_3 - r_D(1 - x_2 - x_3))\phi_V^s(x_3) \\ &\quad - (x_1 - x_3 + r_D(1 - 2x_1 - x_2 + x_3))\phi_V^t(x_3)]\alpha_s(t_d)h_e(\beta_d, \alpha_e, b_3, b_2) \exp[-S_{cd}(t_d)]\}, \end{aligned} \quad (\text{A8})$$

$$\begin{aligned} \mathcal{M}_e^{\text{LRT}} = \mathcal{M}_e^{\text{LRN}} &= -\frac{8}{3}\pi C_f f_B M_B^4 r_D \int_0^1 dx_2 dx_3 \int_0^\infty b_2 b_3 db_2 db_3 \phi_{D^{(*)}}^*(x_2, b_2) \phi_V^T(x_3)(x_1 + x_2 - 1) \\ &\quad \times \{\alpha_s(t_c)h_e(\beta_c, \alpha_e, b_3, b_2) \exp[-S_{cd}(t_c)] + \alpha_s(t_d)h_e(\beta_d, \alpha_e, b_3, b_2) \exp[-S_{cd}(t_d)]\}, \end{aligned} \quad (\text{A9})$$

$$\begin{aligned}
 \mathcal{M}_e^{\text{SP,L}} &= -\frac{8}{3}\pi C_f f_B M_B^4 \int_0^1 dx_2 dx_3 \int_0^\infty b_2 b_3 db_2 db_3 \phi_{D(s)}^*(x_2, b_2) \phi_V(x_3) \\
 &\quad \times \{[2 - 2x_1 - x_2 - x_3 + r_D(x_1 + x_2 - 1)]\alpha_s(t_c) h_e(\beta_c, \alpha_e, b_3, b_2) \exp[-S_{cd}(t_c)] \\
 &\quad - [x_3 - x_1 - r_D(x_1 + x_2 - 1)]\alpha_s(t_d) h_e(\beta_d, \alpha_e, b_3, b_2) \exp[-S_{cd}(t_d)]\}, \tag{A10}
 \end{aligned}$$

$$\begin{aligned}
 \mathcal{M}_e^{\text{SP,N}} &= -\frac{8}{3}\pi C_f f_B M_B^4 r_V \int_0^1 dx_2 dx_3 \int_0^\infty b_2 b_3 db_2 db_3 \phi_{D(s)}^*(x_2, b_2) \{[(x_1 + x_3 - 1 - 2r_D(2x_1 + x_2 + x_3 - 2))\phi_V^v(x_3) \\
 &\quad - (x_1 + x_3 - 1)\phi_V^a(x_3)]\alpha_s(t_c) h_e(\beta_c, \alpha_e, b_3, b_2) \exp[-S_{cd}(t_c)] + (x_1 - x_3)(\phi_V^v(x_3) \\
 &\quad - \phi_V^a(x_3))\alpha_s(t_d) h_e(\beta_d, \alpha_e, b_3, b_2) \exp[-S_{cd}(t_d)]\}, \tag{A11}
 \end{aligned}$$

$$\begin{aligned}
 \mathcal{M}_e^{\text{SP,T}} &= \frac{8}{3}\pi C_f f_B M_B^4 r_V \int_0^1 dx_2 dx_3 \int_0^\infty b_2 b_3 db_2 db_3 \phi_{D(s)}^*(x_2, b_2) \{[(x_1 + x_3 - 1 - 2r_D(2x_1 + x_2 + x_3 - 2))\phi_V^a(x_3) \\
 &\quad - (x_1 + x_3 - 1)\phi_V^v(x_3)]\alpha_s(t_c) h_e(\beta_c, \alpha_e, b_3, b_2) \exp[-S_{cd}(t_c)] + (x_1 - x_3)(\phi_V^a(x_3) \\
 &\quad - \phi_V^v(x_3))\alpha_s(t_d) h_e(\beta_d, \alpha_e, b_3, b_2) \exp[-S_{cd}(t_d)]\}, \tag{A12}
 \end{aligned}$$

$$\begin{aligned}
 \mathcal{F}_a^{\text{LL,L}} &= 8C_F f_B \pi M_B^4 \int_0^1 dx_2 dx_3 \int_0^\infty b_2 b_3 db_2 db_3 \phi_{D(s)}^*(x_2, b_2) \\
 &\quad \times \{[-x_3 \phi_V(x_3) + r_c r_V (\phi_V^t(x_3) - \phi_V^s(x_3))]\alpha_s(t_e) h_e(\alpha_a, \beta_e, b_2, b_3) \exp[-S_{ef}(t_e)] S_t(x_3) \\
 &\quad + [x_2 \phi_V(x_3) + 2r_V r_D (x_2 - 1) \phi_V^s(x_3)]\alpha_s(t_f) h_e(\alpha_a, \beta_f, b_3, b_2) \exp[-S_{ef}(t_f)] S_t(x_2)\}, \tag{A13}
 \end{aligned}$$

$$\begin{aligned}
 \mathcal{F}_a^{\text{LL,N}} &= -8C_F f_B \pi M_B^4 r_D \int_0^1 dx_2 dx_3 \int_0^\infty b_2 b_3 db_2 db_3 \phi_{D(s)}^*(x_2, b_2) \{[r_V(x_3 - 1)\phi_V^a(x_3) - r_c \phi_V^T(x_3) \\
 &\quad + r_V(x_3 + 1)\phi_V^v(x_3)]\alpha_s(t_e) h_e(\alpha_a, \beta_e, b_2, b_3) \exp[-S_{ef}(t_e)] S_t(x_3) - r_V[(x_2 + 1)\phi_V^v(x_3) \\
 &\quad - (x_2 - 1)\phi_V^a(x_3)]\alpha_s(t_f) h_e(\alpha_a, \beta_f, b_3, b_2) \exp[-S_{ef}(t_f)] S_t(x_2)\}, \tag{A14}
 \end{aligned}$$

$$\begin{aligned}
 \mathcal{F}_a^{\text{LL,T}} &= 8C_F f_B \pi M_B^4 r_D \int_0^1 dx_2 dx_3 \int_0^\infty b_2 b_3 db_2 db_3 \phi_{D(s)}^*(x_2, b_2) \{[r_V(x_3 + 1)\phi_V^a(x_3) - r_c \phi_V^T(x_3) \\
 &\quad + r_V(x_3 - 1)\phi_V^v(x_3)]\alpha_s(t_e) h_e(\alpha_a, \beta_e, b_2, b_3) \exp[-S_{ef}(t_e)] S_t(x_3) + r_V[(-x_2 - 1)\phi_V^a(x_3) \\
 &\quad + (x_2 - 1)\phi_V^v(x_3)]\alpha_s(t_f) h_e(\alpha_a, \beta_f, b_3, b_2) \exp[-S_{ef}(t_f)] S_t(x_2)\}, \tag{A15}
 \end{aligned}$$

$$\mathcal{F}_a^{\text{LR,L}} = \mathcal{F}_a^{\text{LLL,L}}, \quad \mathcal{F}_a^{\text{LR,N}} = \mathcal{F}_a^{\text{LL,N}}, \quad \mathcal{F}_a^{\text{LR,T}} = \mathcal{F}_a^{\text{LL,T}}, \tag{A16}$$

$$\begin{aligned}
 \mathcal{F}_a^{\text{SP,L}} &= 16C_F f_B \pi M_B^4 \int_0^1 dx_2 dx_3 \int_0^\infty b_2 b_3 db_2 db_3 \phi_{D(s)}^*(x_2, b_2) \{[r_c \phi_V(x_3) + r_V x_3 (\phi_V^s(x_3) \\
 &\quad - \phi_V^t(x_3))]\alpha_s(t_e) h_e(\alpha_a, \beta_e, b_2, b_3) \exp[-S_{ef}(t_e)] - [r_D x_2 \phi_V(x_3) \\
 &\quad - 2r_V \phi_V^s(x_3)]\alpha_s(t_f) h_e(\alpha_a, \beta_f, b_3, b_2) \exp[-S_{ef}(t_f)]\}, \tag{A17}
 \end{aligned}$$

$$\begin{aligned}
 \mathcal{F}_a^{\text{SP,N}} &= -16C_F f_B \pi M_B^4 \int_0^1 dx_2 dx_3 \int_0^\infty b_2 b_3 db_2 db_3 \phi_{D(s)}^*(x_2, b_2) \times \{r_D [\phi_V^T(x_3) - 2r_c r_V \phi_V^v(x_3)]\alpha_s(t_e) h_e(\alpha_a, \beta_e, b_2, b_3) \\
 &\quad \times \exp[-S_{ef}(t_e)] + r_V (\phi_V^v(x_3) + \phi_V^a(x_3))\alpha_s(t_f) h_e(\alpha_a, \beta_f, b_3, b_2) \exp[-S_{ef}(t_f)]\}, \tag{A18}
 \end{aligned}$$

$$\begin{aligned}
 \mathcal{F}_a^{\text{SP,T}} &= -16C_F f_B \pi M_B^4 \int_0^1 dx_2 dx_3 \int_0^\infty b_2 b_3 db_2 db_3 \phi_{D(s)}^*(x_2, b_2) \times \{r_D [\phi_V^T(x_3) - 2r_c r_V \phi_V^a(x_3)]\alpha_s(t_e) h_e(\alpha_a, \beta_e, b_2, b_3) \\
 &\quad \times \exp[-S_{ef}(t_e)] + r_V (\phi_V^v(x_3) + \phi_V^a(x_3))\alpha_s(t_f) h_e(\alpha_a, \beta_f, b_3, b_2) \exp[-S_{ef}(t_f)]\}, \tag{A19}
 \end{aligned}$$

$$\begin{aligned} \mathcal{M}_a^{\text{LL,L}} = & \frac{8}{3} C_F f_B \pi M_B^4 \int_0^1 dx_2 dx_3 \int_0^\infty b_1 b_2 db_1 db_2 \phi_{D_{(s)}^*}(x_2, b_2) \{ [(x_1 - x_2 - r_c) \phi_V(x_3) - r_D r_V [(x_2 - x_3) \phi_V^s(x_3) \\ & - (2x_1 - x_2 - x_3) \phi_V^t(x_3)]] \alpha_s(t_g) h_e(\beta_g, \alpha_a, b_1, b_2) \exp[-S_{gh}(t_g)] - [(1 - r_b - x_1 - x_3) \phi_V(x_3) \\ & - r_D r_V [(x_3 - x_2) \phi_V^s(x_3) + (2x_1 + x_2 + x_3 - 2) \phi_V^t(x_3)]] \alpha_s(t_h) h_e(\beta_h, \alpha_a, b_1, b_2) \exp[-S_{gh}(t_h)] \}, \end{aligned} \quad (\text{A20})$$

$$\begin{aligned} \mathcal{M}_a^{\text{LL,N}} = & -\frac{16}{3} C_F f_B \pi M_B^4 r_D r_V \int_0^1 dx_2 dx_3 \int_0^\infty b_1 b_2 db_1 db_2 \phi_{D_{(s)}^*}(x_2, b_2) \phi_V^v(x_3) \{ r_c \alpha_s(t_g) h_e(\beta_g, \alpha_a, b_1, b_2) \\ & \times \exp[-S_{gh}(t_g)] - r_b \alpha_s(t_h) h_e(\beta_h, \alpha_a, b_1, b_2) \exp[-S_{gh}(t_h)] \}, \end{aligned} \quad (\text{A21})$$

$$\begin{aligned} \mathcal{M}_a^{\text{LL,T}} = & -\frac{16}{3} C_F f_B \pi M_B^4 r_D r_V \int_0^1 dx_2 dx_3 \int_0^\infty b_1 b_2 db_1 db_2 \phi_{D_{(s)}^*}(x_2, b_2) \phi_V^a(x_3) \{ r_c \alpha_s(t_g) h_e(\beta_g, \alpha_a, b_1, b_2) \\ & \times \exp[-S_{gh}(t_g)] - r_b \alpha_s(t_h) h_e(\beta_h, \alpha_a, b_1, b_2) \exp[-S_{gh}(t_h)] \}, \end{aligned} \quad (\text{A22})$$

$$\begin{aligned} \mathcal{M}_a^{\text{LR,L}} = & \frac{8}{3} C_F f_B \pi M_B^4 \int_0^1 dx_2 dx_3 \int_0^\infty b_1 b_2 db_1 db_2 \phi_{D_{(s)}^*}(x_2, b_2) \{ [r_D(x_1 - x_2 + r_c) \phi_V(x_3) + r_V(-x_1 + x_3 - r_c) (\phi_V^s(x_3) \\ & + \phi_V^t(x_3))] \alpha_s(t_g) h_e(\beta_g, \alpha_a, b_1, b_2) \exp[-S_{gh}(t_g)] - [-r_D(x_1 + x_2 - r_b - 1) \phi_V(x_3) \\ & + r_V(x_1 + x_3 - r_b - 1) (\phi_V^s(x_3) + \phi_V^t(x_3))] \alpha_s(t_h) h_e(\beta_h, \alpha_a, b_1, b_2) \exp[-S_{gh}(t_h)] \}, \end{aligned} \quad (\text{A23})$$

$$\begin{aligned} \mathcal{M}_a^{\text{LR,T}} = \mathcal{M}_a^{\text{LR,N}} = & \frac{8}{3} C_F f_B \pi M_B^4 \int_0^1 dx_2 dx_3 \int_0^\infty b_1 b_2 db_1 db_2 \phi_{D_{(s)}^*}(x_2, b_2) \times \{ [r_V(x_1 - x_3 + r_c) (\phi_V^v(x_3) + \phi_V^a(x_3)) \\ & - r_D(x_1 - x_2 + r_c) \phi_V^T(x_3)] \alpha_s(t_g) h_e(\beta_g, \alpha_a, b_1, b_2) \exp[-S_{gh}(t_g)] + [r_V(x_1 + x_3 - r_b - 1) (\phi_V^v(x_3) \\ & + \phi_V^a(x_3)) + r_D(1 + r_b - x_1 - x_2) \phi_V^T(x_3)] \alpha_s(t_h) h_e(\beta_h, \alpha_a, b_1, b_2) \exp[-S_{gh}(t_h)] \}, \end{aligned} \quad (\text{A24})$$

$$\begin{aligned} \mathcal{M}_a^{\text{SP,L}} = & \frac{8}{3} C_F f_B \pi M_B^4 \int_0^1 dx_2 dx_3 \int_0^\infty b_1 b_2 db_1 db_2 \phi_{D_{(s)}^*}(x_2, b_2) \{ [(x_1 - x_3 - r_c) \phi_V(x_3) - r_D r_V [(x_3 - x_2) \phi_V^s(x_3) \\ & - (2x_1 - x_2 - x_3) \phi_V^t(x_3)]] \alpha_s(t_g) h_e(\beta_g, \alpha_a, b_1, b_2) \exp[-S_{gh}(t_g)] - [(1 - r_b - x_1 - x_2) \phi_V(x_3) \\ & - r_D r_V [(x_2 - x_3) \phi_V^s(x_3) + (2x_1 + x_2 + x_3 - 2) \phi_V^t(x_3)]] \alpha_s(t_h) h_e(\beta_h, \alpha_a, b_1, b_2) \exp[-S_{gh}(t_h)] \}, \end{aligned} \quad (\text{A25})$$

$$\mathcal{M}_a^{\text{SP,N}} = \mathcal{M}_a^{\text{LL,N}}, \quad \mathcal{M}_a^{\text{SP,T}} = -\mathcal{M}_a^{\text{LL,T}}. \quad (\text{A26})$$

## APPENDIX B: SCALES AND RELATED FUNCTIONS IN HARD KERNEL

We show here the functions  $h_e$ , coming from the Fourier transform of the hard kernel.

$$\begin{aligned} h_e(\alpha, \beta, b_1, b_2) = h_1(\alpha, b_1) \times h_2(\beta, b_1, b_2), \quad h_1(\alpha, b_1) = & \begin{cases} K_0(\sqrt{\alpha} b_1), & \alpha > 0 \\ K_0(i\sqrt{-\alpha} b_1), & \alpha < 0 \end{cases} \\ h_2(\beta, b_1, b_2) = & \begin{cases} \theta(b_1 - b_2) I_0(\sqrt{\beta} b_2) K_0(\sqrt{\beta} b_1) + (b_1 \leftrightarrow b_2), & \beta > 0 \\ \theta(b_1 - b_2) J_0(\sqrt{-\beta} b_2) K_0(i\sqrt{-\beta} b_1) + (b_1 \leftrightarrow b_2), & \beta < 0 \end{cases} \end{aligned} \quad (\text{B1})$$

where  $J_0$  is the Bessel function and  $K_0, I_0$  are modified Bessel functions with  $K_0(ix) = \frac{\pi}{2}(-N_0(x) + iJ_0(x))$ . The hard scale  $t$  is chosen as the maximum of the virtuality of the internal momentum transition in the hard amplitudes, including  $1/b_i (i = 1, 2, 3)$ :

$$\begin{aligned} t_a = \max(\sqrt{|\alpha_e|}, \sqrt{|\beta_a|}, 1/b_1, 1/b_2), \quad t_b = \max(\sqrt{|\alpha_e|}, \sqrt{|\beta_b|}, 1/b_1, 1/b_2), \quad t_c = \max(\sqrt{|\alpha_e|}, \sqrt{|\beta_c|}, 1/b_2, 1/b_3), \\ t_d = \max(\sqrt{|\alpha_e|}, \sqrt{|\beta_d|}, 1/b_2, 1/b_3), \quad t_e = \max(\sqrt{|\alpha_a|}, \sqrt{|\beta_e|}, 1/b_2, 1/b_3), \quad t_f = \max(\sqrt{|\alpha_a|}, \sqrt{|\beta_f|}, 1/b_2, 1/b_3), \\ t_g = \max(\sqrt{|\alpha_a|}, \sqrt{|\beta_g|}, 1/b_1, 1/b_2), \quad t_h = \max(\sqrt{|\alpha_a|}, \sqrt{|\beta_h|}, 1/b_1, 1/b_2), \end{aligned} \quad (\text{B2})$$

where

$$\begin{aligned}
\alpha_e &= (1 - x_1 - x_2)(x_1 - r_D^2)M_B^2, & \alpha_a &= -x_2x_3(1 - r_D^2)M_B^2, & \beta_a &= [r_b^2 - x_2(1 - r_D^2)]M_B^2, \\
\beta_b &= -(1 - x_1)(x_1 - r_D^2)M_B^2, & \beta_c &= -(1 - x_1 - x_2)[1 - x_1 - x_3(1 - r_D^2)]M_B^2, \\
\beta_d &= (1 - x_1 - x_2)[x_1 - x_3 - r_D^2(1 - x_3)]M_B^2, & \beta_e &= [r_c^2 - x_3 - (1 - x_3)r_D^2]M_B^2, & \beta_f &= -x_2(1 - r_D^2)M_B^2, \\
\beta_g &= [r_c^2 - (x_1 - x_3(1 - r_D^2))(x_1 - x_2)]M_B^2, & \beta_h &= [r_b^2 - (1 - x_1 - x_3 + x_3r_D^2)(1 - x_1 - x_2)]M_B^2.
\end{aligned} \tag{B3}$$

The Sudakov factors used in the text are defined by

$$\begin{aligned}
S_{ab}(t) &= s\left(\frac{M_B}{\sqrt{2}}x_1, b_1\right) + s\left(\frac{M_B}{\sqrt{2}}x_2, b_2\right) + \frac{5}{3} \int_{1/b_1}^t \frac{d\mu}{\mu} \gamma_q(\mu) + 2 \int_{1/b_2}^t \frac{d\mu}{\mu} \gamma_q(\mu), \\
S_{cd}(t) &= s\left(\frac{M_B}{\sqrt{2}}x_1, b_2\right) + s\left(\frac{M_B}{\sqrt{2}}x_2, b_2\right) + s\left(\frac{M_B}{\sqrt{2}}x_3, b_3\right) + s\left(\frac{M_B}{\sqrt{2}}(1 - x_3), b_3\right) + \frac{11}{3} \int_{1/b_2}^t \frac{d\mu}{\mu} \gamma_q(\mu) + 2 \int_{1/b_3}^t \frac{d\mu}{\mu} \gamma_q(\mu), \\
S_{ef}(t) &= s\left(\frac{M_B}{\sqrt{2}}x_2, b_2\right) + s\left(\frac{M_B}{\sqrt{2}}x_3, b_3\right) + s\left(\frac{M_B}{\sqrt{2}}(1 - x_3), b_3\right) + 2 \int_{1/b_2}^t \frac{d\mu}{\mu} \gamma_q(\mu) + 2 \int_{1/b_3}^t \frac{d\mu}{\mu} \gamma_q(\mu), \\
S_{gh}(t) &= s\left(\frac{M_B}{\sqrt{2}}x_1, b_1\right) + s\left(\frac{M_B}{\sqrt{2}}x_2, b_2\right) + s\left(\frac{M_B}{\sqrt{2}}x_3, b_2\right) + s\left(\frac{M_B}{\sqrt{2}}(1 - x_3), b_2\right) + \frac{5}{3} \int_{1/b_1}^t \frac{d\mu}{\mu} \gamma_q(\mu) + 4 \int_{1/b_2}^t \frac{d\mu}{\mu} \gamma_q(\mu),
\end{aligned} \tag{B4}$$

where the functions  $s(Q, b)$  are defined in Appendix A of Ref. [8].  $\gamma_q = -\alpha_s/\pi$  is the anomalous dimension of the quark.

### APPENDIX C: LIGHT-CONE DISTRIBUTION AMPLITUDES

Here, we specify the light-cone distribution amplitudes for pseudoscalar and vector mesons. The expressions of twist-2 light-cone distribution amplitudes are [7]

$$\begin{aligned}
\phi_P^A(x) &= \frac{f_P}{\sqrt{6}} 3x(1-x)[1 + a_1^P C_1^{3/2}(t) + a_2^P C_2^{3/2}(t) + a_4^P C_4^{3/2}(t)], \\
\phi_V(x) &= \frac{f_V}{\sqrt{6}} 3x(1-x)[1 + a_{1V}^{\parallel} C_1^{3/2}(t) + a_{2V}^{\parallel} C_2^{3/2}(t)], \\
\phi_V^T(x) &= \frac{f_V^T}{\sqrt{6}} 3x(1-x)[1 + a_{1V}^{\perp} C_1^{3/2}(t) + a_{2V}^{\perp} C_2^{3/2}(t)],
\end{aligned} \tag{C1}$$

and those of twist-3 ones are

$$\begin{aligned}
\phi_P^P(x) &= \frac{f_P}{2\sqrt{6}} \left[ 1 + \left( 30\eta_3 - \frac{5}{2}\rho_P^2 \right) C_2^{1/2}(t) - \left( \eta_3\omega_3 + \frac{9}{20}\rho_P^2(1 + 6a_P^2) \right) C_4^{1/2}(t) \right], \\
\phi_P^t(x) &= \frac{f_P}{2\sqrt{6}} \left[ 1 + 6 \left( 5\eta_3 - \frac{1}{2}\eta_3\omega_3 - \frac{7}{20}\rho_P^2 - \frac{3}{5}\rho_P^2 a_P^2 \right) (1 - 10x + 10x^2) \right], & \phi_V^T(x) &= \frac{3f_V^T}{2\sqrt{6}} t^2, \\
\phi_V^s(x) &= -\frac{3f_V^T}{2\sqrt{6}} t, & \phi_V^v(x) &= \frac{3f_V^T}{8\sqrt{6}} (1 + t^2), & \phi_V^a(x) &= -\frac{3f_V^T}{4\sqrt{6}} t,
\end{aligned} \tag{C2}$$

where  $t = 2x - 1$ ,  $f_V$  and  $f_V^T$  are the decay constants of the vector meson with longitudinal and transverse polarization, respectively. For all pseudoscalar mesons, we choose  $\eta_3 = 0.015$  and  $\omega_3 = -3$  [26]. The mass ratio  $\rho_{\pi(K)} = m_{\pi(K)}/m_0^{\pi(K)}$  and  $\rho_{\eta_q(s)} = 2m_{q(s)}/m_{qq(ss)}$ , and the Gegenbauer polynomials  $C_n^{\nu}(t)$  read

$$\begin{aligned}
C_2^{1/2}(t) &= \frac{1}{2}(3t^2 - 1), & C_4^{1/2}(t) &= \frac{1}{8}(3 - 30t^2 + 35t^4), & C_1^{3/2}(t) &= 3t, \\
C_2^{3/2}(t) &= \frac{3}{2}(5t^2 - 1), & C_4^{3/2}(t) &= \frac{15}{8}(1 - 14t^2 + 21t^4).
\end{aligned} \tag{C3}$$

- [1] N. Brambilla *et al.* (Quarkonium Working Group), Report No. CERN-2005-005.
- [2] D.-S. Du and Z. Wang, *Phys. Rev. D* **39**, 1342 (1989).
- [3] H.-M. Choi and C.-R. Ji, *Phys. Rev. D* **80**, 114003 (2009).
- [4] H.-M. Choi and C.-R. Ji, *Phys. Rev. D* **80**, 054016 (2009).
- [5] J.-F. Liu and K.-T. Chao, *Phys. Rev. D* **56**, 4133 (1997); M. A. Ivanov, J. G. Korner, and P. Santorelli, *Phys. Rev. D* **73**, 054024 (2006).
- [6] J. Sun, Y. Yang, W. Du, and H. Ma, *Phys. Rev. D* **77**, 114004 (2008).
- [7] X. Liu, Z.-J. Xiao, and C.-D. Lü, *Phys. Rev. D* **81**, 014022 (2010).
- [8] J.-F. Cheng, D.-S. Du, and C.-D. Lü, *Eur. Phys. J. C* **45**, 711 (2006).
- [9] J. Sun, D.-s. Du, and Y. Yang, *Eur. Phys. J. C* **60**, 107 (2009).
- [10] J. Zhang and X.-Q. Yu, *Eur. Phys. J. C* **63**, 435 (2009).
- [11] H.-Y. Cheng and C.-K. Chua, *Phys. Rev. D* **80**, 114008 (2009).
- [12] D.-S. Du and Z.-T. Wei, *Eur. Phys. J. C* **5**, 705 (1998).
- [13] Z.-J. Xiao and X. Liu, *Phys. Rev. D* **84**, 074033 (2011).
- [14] Y. Y. Keum, H. n. Li, and A. I. Sanda, *Phys. Lett. B* **504**, 6 (2001); C.-D. Lü, K. Ukai, and M. Z. Yang, *Phys. Rev. D* **63**, 074009 (2001); C.-D. Lü and M. Z. Yang, *Eur. Phys. J. B* **23**, 275 (2002).
- [15] B. H. Hong and C. D. Lu, *Sci. China G* **49**, 357 (2006).
- [16] R.-H. Li, C.-D. Lü, and H. Zou, *Phys. Rev. D* **78**, 014018 (2008); R.-H. Li, C.-D. Lü, A. I. Sanda, and X.-X. Wang, *Phys. Rev. D* **81**, 034006 (2010).
- [17] H. Zou, R.-H. Li, X.-X. Wang, and C.-D. Lü, *J. Phys. G* **37**, 015002 (2010).
- [18] Y. Li, C.-D. Lü, and C.-F. Qiao, *Phys. Rev. D* **73**, 094006 (2006); Y. Li and C.-D. Lü, *J. Phys. G* **29**, 2115 (2003); Y. Li, C.-D. Lü, and Z.-J. Xiao, *J. Phys. G* **31**, 273 (2005).
- [19] Y.-Y. Keum, T. Kurimoto, H. Li, C.-D. Lü, and A. I. Sanda, *Phys. Rev. D* **69**, 094018 (2004).
- [20] C.-D. Lü, *Eur. Phys. J. C* **24**, 121 (2002).
- [21] T. Kurimoto, H. n. Li, and A. I. Sanda, *Phys. Rev. D* **67**, 054028 (2003).
- [22] G. Buchalla, A. J. Buras, and M. E. Lautenbacher, *Rev. Mod. Phys.* **68**, 1125 (1996).
- [23] M. Beneke, G. Buchalla, M. Neubert, and C. T. Sachrajda, *Phys. Rev. Lett.* **83**, 1914 (1999); *Nucl. Phys.* **B591**, 313 (2000).
- [24] C. W. Bauer, S. Fleming, D. Pirjol, and I. W. Stewart, *Phys. Rev. D* **63**, 114020 (2001); C. W. Bauer, D. Pirjol, and I. W. Stewart, *Phys. Rev. Lett.* **87**, 201806 (2001).
- [25] J. C. Collins and D. E. Soper, *Nucl. Phys.* **B193**, 381 (1981); J. Botts and G. Sterman, *Nucl. Phys.* **B325**, 62 (1989).
- [26] V. M. Braun and I. E. Filyanov, *Z. Phys. C* **48**, 239 (1990); P. Ball, V. M. Braun, Y. Koike, and K. Tanaka, *Nucl. Phys.* **B529**, 323 (1998); P. Ball, *J. High Energy Phys.* 01 (1999) 010.
- [27] C.-D. Lü and M.-Z. Yang, *Eur. Phys. J. C* **28**, 515 (2003).
- [28] A. V. Manohar and M. B. Wise, Cambridge Monogr. Part. Phys., Nucl. Phys., Cosmol. **10**, 1 (2000).
- [29] B. Melic, B. Nizic, and K. Passek, *Phys. Rev. D* **60**, 074004 (1999).
- [30] P. Ball and R. Zwicky, *Phys. Rev. D* **71**, 014015 (2005); *J. High Energy Phys.* 04 (2006) 046; P. Ball and G. W. Jones, *J. High Energy Phys.* 03 (2007) 069.
- [31] Th. Feldmann, P. Kroll, and B. Stech, *Phys. Rev. D* **58**, 114006 (1998).
- [32] R. Escribano and J. M. Frere, *J. High Energy Phys.* 06 (2005) 029; J. Schechter, A. Subbaraman, and H. Weigel, *Phys. Rev. D* **48**, 339 (1993).
- [33] Particle Data Group, *J. Phys. G* **37**, 075021 (2010).
- [34] W. Wang, Y.-L. Shen, and C.-D. Lu, *Phys. Rev. D* **79**, 054012 (2009).
- [35] A. Ali, G. Kramer, and C.-D. Lü, *Phys. Rev. D* **58**, 094009 (1998); Y.-H. Chen, H.-Y. Cheng, B. Tseng, and K.-C. Yang, *Phys. Rev. D* **60**, 094014 (1999).
- [36] S. Descotes-Genon, J. He, E. Kou, and P. Robbe, *Phys. Rev. D* **80**, 114031 (2009).
- [37] Y. Li and C.-D. Lü, *Phys. Rev. D* **73**, 014024 (2006).
- [38] C.-H. Chen, Y.-Y. Keum, and H.-N. Li, *Phys. Rev. D* **66**, 054013 (2002).
- [39] H.-W. Huang, C.-D. Lü, T. Morii, Y.-L. Shen, G.-L. Songe, and J. Zhu, *Phys. Rev. D* **73**, 014011 (2006).